NAVAL POSTGRADUATE SCHOOL
Monterey, California

THESIS

ELECTRODYNAMIC BEHAVIOR
OF PMG-DELTA

by

Chang, Chung-Jen

June 1994

Thesis Advisor: Richard Christopher Olsen
Second Reader: Suntharalingam Gnanalingam

REPORT DOCUMENTATION PAGE

Form approved OMB No. 0704-188

1. AGENCY USE ONLY (*Leave Blank*)	2. REPORT DATE	3. REPORT TYPE AND DATES COVERED
	June 1994	Master's Thesis

4. TITLE AND SUBTITLE
ELECTRODYNAMIC BEHAVIOR OF PMG-DELTA

5. FUNDING NUMBERS

6. AUTHOR(S)
CHANG, CHUNG-JEN

7. PERFORMING ORGANIZATION NAME(S) AND ADDRESS(ES)
Naval Postgraduate School
Monterey, CA 93943-5000

8. PERFORMING ORGANIZATION REPORT NUMBER

9. SPONSORING/MONITORING AGENCY NAME(S) AND ADDRESS(ES)

10. SPONSORING/MONITORING AGENCY REPORT NUMBER

11. SUPPLEMENTARY NOTES

The views expressed in this thesis are those of the author and do not reflect the official policy or position of the Department of Defense or the U.S. Government

12a. DISTRIBUTION/AVAILABILITY STATEMENT
Approved for public release; distribution is unlimited.

12b. DISTRIBUTION CODE

13. ABSTRACT (Maximum 200 words)

The PMG-Delta experimant was launched on 26 June 1993 to test basic tether electrodynamic principles. The 500 m conducting tether deployed from the second stage of a Delta-rocket, and provided ~3 orbits of useful information. The tether was equipped at both ends with xenon hollow cathodes. With both cathodes operating, currents up to 0.3A could be driven in either direction. Plasma impedances outside the tether were as low as a few hundred ohms at peak current during daytime/perigee(200km). Large impedances (10~100kΩ) occurred at night/apogee(900km), or when cathode cycled off.

14. SUBJECT TERMS
Organizational Learning, Lessons Learned, After Action Reports, Information Systems

15. NUMBER OF PAGES
73

16. PRICE CODE

17. SECURITY CLASSIFICATION OF REPORT	18. SECURITY CLASSIFICATION OF THIS PAGE	19. SECURITY CLASSIFICATION OF THIS ABSTRACT	20. LIMITATION OF ABSTRACT
Unclassified	Unclassified	Unclassified	UL

NSN 7540-01-280-5500

Standard Form 298 (Rev. 2-89)
Prescribed by ANSI Std 239-18

Approved for public release; distribution is unlimited.

ELECTRODYNAMIC BEHAVIOR OF PMG-DELTA

by

Chang, Chung-Jen
Lieutenant Commander, Taiwan, R.O.C. Navy
B.S., Chinese Naval Academy, 1979

Submitted in partial fulfillment
of the requirements for the degree of

MASTER OF SCIENCE IN ENGINEERING ACOUSTICS

from the
NAVAL POSTGRADUATE SCHOOL

June 1994

Author: Chang, Chung-Jen

Approved by: Richard Christopher Olsen, Thesis Advisor

Suntharalingam Gnanalingam, Second Reader

W. B. Colson
William Boniface Colson, Chairman
Department of Physics

ABSTRACT

The PMG-Delta experiment was launched on 26 June 1993 to test basic tether electrodynamic principles. The 500 m conducting tether deployed from the second stage of a Delta-rocket, and provided ~3 orbits of useful information. The tether was equipped at both ends with xenon hollow cathodes. With both cathodes operating, currents up to 0.3 A could be driven in either direction. Plasma impedances outside the tether were as low as a few hundred ohms at peak current during daytime/perigee (200 km). Large impedances (10~100 kΩ) occurred at night/apogee (900 km), or when one cathode cycled off.

TABLE OF CONTENTS

I. INTRODUCTION 1

II. BACKGROUND 3

A. THE ENVIRONMENT OF THE EXPERIMENT. 3

B. GEMINI 3

C. TETHER SATELLITE SYSTEM. 4

D. THE HOLLOW CATHODE 5

E. SEDS 6

III. THE PLASMA-MOTOR-GENERATOR EXPERIMENT 8

IV. OBSERVATION 12

A. DEPLOYMENT 12

B. STANDARD MODES 12

1. Tether current depends on environment 13

C. THE EFFECTS OF HOLLOW CATHODE. 15

D. SYSTEM IMPEDANCE 19

1. Plasma impedance. 20

V. SUMMARY AND CONCLUSIONS 21

LIST OF REFERENCES 61

INITIAL DISTRIBUTION LIST. 62

LIST OF TABLES

Table 1. THE PMG ON-ORBIT EVENT TIMELINE. 9

Table 2. HOLLOW CATHODE "ON","OFF" TIMING 15

LIST OF FIGURES

Figure 1. Plasma density with altitude in the ionosphere. . . 23

Figure 2. Gemini spacecraft tethered configuration. 24

Figure 3. TSS operation concept 25

Figure 4. TSS configuration in cargo bay. 26

Figure 5. Shuttle-tether-satellite sketch. 27

Figure 6. TSS around Earth's ionosphere as moving conductor . 28

Figure 7. TSS-1, deployed satellite 29

Figure 8. Plasma-bridge neutralizer cathode construction. . . 30

Figure 9. Hollow Cathode Assembly configuration 31

Figure 10. SEDS arrangement inside Delta II second stage . . . 32

Figure 11. SEDS location on Delta II launch vehicle. 33

Figure 12. Delta second stage with deployed tether 34

Figure 13. PMG demonstration of electrodynamic tether principles. 35

Figure 14. Location of PMG package on Delta second stage . . . 36

Figure 15. PMG mechanical layout 37

Figure 16. NEP anode voltage with timing 38

Figure 17. Altitude of Orbiter 39

Figure 18. Orbiter track diagram 40

Figure 19. PMG circuit diagram 41

Figure 20. Standard data frame sequence. 42

Figure 21. PMG-Delta deployment phase. 43

Figure 22. Data frame 80 44

Figure 23. Data frame 4. 45

Figure 24. Data frame 9. 46
Figure 25. Data frame 83 47
Figure 26. Data frame 85 48
Figure 27. Data frame 145. 49
Figure 28. Potential summary 50
Figure 29. Current summary 51
Figure 30. Current change with FEP/HCA working state 52
Figure 31. Current change with FEP/HCA working state 53
Figure 32. No current change with FEP/HCA working state. . . . 54
Figure 33. Potential change with HCA working condition 55
Figure 34. Potential change with HCA working condition 56
Figure 35. Potential change with HCA working condition 57
Figure 36. Plasma impedance at different bias voltage and load resistance 58
Figure 37. Plasma impedance at different bias voltage and load resistance 59
Figure 38. Impedance with current. 60
Figure 39. Impedance with current. 61

ACKNOWLEDGMENTS

Thanks to Dr. Jim McCoy principal investigator for PMG-Delta, for bringing the project to completion. I wish to express my thanks to my Thesis Advisor, Dr. Richard Christopher Olsen, for his understanding, infinite patience, and guidance. I would also like to thank Dr. Suntharalingam Gnanalingam, who provided a lot of help and enthusiasm when it was greatly needed. Last, but by no means least, I would like to extend deep appreciation to my family and friends who gave their total support throughout the entire project.

I. INTRODUCTION

The electrodynamic tether is, at its most basic level, a wire moving through a magnetic field. The relationship between the resulting electric field, currents, and forces has fascinated physicists since the days of Oersted in 1820.[*Ref. 1: p. 636*] Space tethers emerged as a concept in the early 1970's with the work by Mario Grossi, and with encouragement of Hannes Alfven. A long wire in space, anchored (or not) at the ends with satellites, is a stable system, due to gravity gradient effects.[*Ref. 2*] As such, an electrodynamic tether offers intriguing possibilities as both a motor and generator.

For the propose of studying these phenomena, a joint venture of the United States' National Aeronautics and Space Administration (NASA) and Italy's Agenzia Spaziale Italiana (ASI, the Italian Space Agency) developed the Tethered Satellite System (TSS-1).

In July 1992, the shuttle deployed a heavily instrumented satellite as a test of tether electrodynamics. Unfortunately, the 20 km cable jammed at 570 feet (USA Today, Aug 5,1992). Relatively low voltages were induced (~40 V) and the corresponding currents were low.(15 mA)(AW&ST, August 10,1992) One reason for low currents in such a system is poor electrical contact with the local plasma environment.

The plasma motor generator experiment, PMG-Delta, was designed to study this electrical connectivity problem. Using Xenon based hollow cathodes also termed plasma contactors,[*Ref. 3*] the 500-m

tether system was deployed from the second stage of a Delta-rocket.

The work which follows considers the electrodynamic behavior of the system.

II. BACKGROUND

A. THE ENVIRONMENT OF THE EXPERIMENT

The upper layer of Earth's electrically neutral atmosphere where the experiment took place, is characterized by the presence of electrically charged gases, or plasma. This region, which extends from 85 km to approximately 1,000 km, is known as the ionosphere. The boundaries of the ionosphere vary according to solar activity. In sunlight, gases in the atmosphere will be ionized by the radiation from the Sun. Once an atom is ionized, it remains charged until it meets an electron; it then very likely recombines with an electron to become neutral again. In darkness the density of ionized gas will be lower. Ionized particles will drift due to effects of the magnetic field and electric fields.

Above the ionosphere is the magnetosphere, which extends from 1,000 km to 60,000 km on the side toward the Sun, and trails out more than 300,000 km away from the Sun. The magnetosphere is the region surrounding Earth in which the geomagnetic field plays a dominant role in the behavior of charged particles.[*Ref. 4*]

Figure 1 shows the variation in plasma density with altitude in the ionosphere.[*Ref. 5: P. 128*] The big difference between day and night is important in our experiment.

B. GEMINI

The first tether in space experiments took place in September and November of 1966. The Gemini XI and XII spacecraft together

with the Atlas-Agena D spent stage performed these experiments.

Figure 2 shows the simple connection of Gemini spacecraft/target-vehicle tethered configuration. In Gemini program, one mode of operation consisted of intentionally inducing an angular velocity in the tethered system by translational thrusting with the spacecraft propulsion system. The other mode involved tethered, drifting flight during which the effect of gravity gradient on the motion of the system was of interest. Those two modes of tethered vehicle operation were completely successful.[*Ref. 6*]

C. TETHERED SATELLITE SYSTEM

The next major tether experiment was TSS-1. The Tethered Satellite System has five major components: the deployer system, the tether, the satellite, the carriers on which the system is mounted, and science instruments. Figure 3 shows the rough configuration of the shuttle, with the deployer extended. Figure 4 shows the shuttle bay prior to extension of the deployer.[*Ref.* 7) Figure 5 shows the 1200 pound Italian satellite in an artist's sketch.(Huntsvile Times, July 27,1992)

The physics of the system is simple. As illustrated in Figure 6, the orbital motion of the deployed system results in an electrical field of the order of 200 V/km along the tether. The resulting potential difference between the ends of the tether will nominally cause the far ends to float positive and negative, with respect to the plasma at the ends of the tether. Hence, charges of

the appropriate sign will flow to the orbiter and satellite, and a net current will flow through the tether.

In order for a complete circuit to exist, current must flow through the plasma. It is difficult for the highly magnetized plasma to conduct such currents, and it is believed that closure may occur via currents along magnetic field lines down into the E-region where collisions allow currents to flow perpendicular to the magnetic field.

In July 1992, TSS-1 was launched on STS-46. Everything worked reasonably well, until ~175 m out, when the cable snagged. Figure 7 shows the deployed satellite. (USA Today, August 5, 1992) The relatively short deployment restricted the V×B induced potential drop to ~40 V, and the resulting currents only reached ~15 mA. (AW&ST, August 10,1992)

The mission was successful, however ,in demonstrating successful (dynamic) control of the satellite, alleviating many fears about the mechanical behavior of the tethers. A reflight is planned for 1995.

D. THE HOLLOW CATHODE

One reason for relatively low currents in the TSS-1 mission may have been relatively high impedances at the satellite-plasma boundaries. One way to deal with this problem is to put plasma sources on the satellites. Gas discharge plasma generators, such as hollow cathodes, can provide an electrical bridge to the more

diffuse ionospheric plasma.[*Ref 8*] Such devices have been termed 'Plasma Contactors'. A major purpose of the PMG-Delta experiment was to test this technology, as applied to a tether system.

Hollow Cathodes, in space applications, have their origins in ion engine technology.[*Ref 9, 10*] Figure 8 shows an early design, due to Rawlin and Pawlik(1968). The primary change since that time has been the transition from rolled foil inserts to porous tungsten inserts, impregnated with barium carbonate ($Ba\ CO_3$).

The Hollow cathode design used for PMG provides a supply of Xenon gas within a hollow electron emitter cathode heated to approximately 1300°C. A strong voltage gradient between the cathode and corresponding anode plate establishes a plasma discharge to create a partially ionized gas. The free expansion of this ionized gas plume from the Hollow Cathode Assembly (HCA) into the surrounding ionosphere creates a region of increased plasma conductivity extending many meters into the ambient plasma. The HCA system configuration is illustrated in Figure 9.

E. SEDS

In the Tethered Satellite System, the deployer is the Small Expendable-tether Deployer System (SEDS), whose design is due to Joe Carroll. This design flew once previous to PMG-Delta, as a non-conducting tether, also successfully deployed from a Delta second stage on March 29, 1993. It has subsequently been flown again, on March 9, 1994.

The concept of SEDS design are: simplicity, non-retrievability, low tension, minimum braking, and a wide swing. The SEDS consists of four key components: the tether wrapped on a aluminum core and located in a canister; the brake/cutter assembly; the endmass (or payload); and the electronics control and data system. Figure 10 shows each component of SEDS arrangement inside Delta II second stage. Figure 11 illustrates the SEDS location on Delta II launch vehicle. Figure 12 shows the Delta second stage with deployed tether.[*Ref. 11, 12*]

III. THE PLASMA-MOTOR-GENERATOR EXPERIMENT

The primary objective of the PMG-Delta flight experiment was to verify the ability of hollow cathode plasma sources to couple electrical currents from either end of a long wire to the ionospheric plasma in Low Earth Orbit (LEO).

The PMG flight hardware consisted of four major subsystems: the Far End Package (FEP), Near End Package (NEP), electronics box, and Plasma Diagnostics Package (PDP). Figure 13 shows the system deployed, with the electrical dynamics of motor and generator modes shown. The deployer is the SEDS design described in the previous section.

The mechanical layout for the PMG experiment is illustrated in Figures 14 and 15 . Note that the dimensions are of order ~12 inches.

This assembly was carried aboard an Air Force Delta-II rocket and launched on June 26, 1993 at 13:27 GMT. After separation, the PMG system was left in an elliptical orbit (207×922 km) at 25.7° inclination. Twenty six minutes later, the PMG system was powered on by automatic command. The FEP was deployed 400 seconds later and subsequently stabilized above the NEP via an 18-AWG 500-meter copper-wire tether.

Table 1, from the PMG mission report (Jost and Stanley,1994) shows the timeline of important events. In addition to the events listed here, the NEP hollow cathode changed mode at 01:00:50, apparently from spot to plume mode (Figure 16). This change was

anticipated, and is a result of the gradual drop in gas pressure in the supply.

Table 1. PMG on-orbit event timeline

EVENT	EVENT ID	PMGT (sec)	GMT (hh:mm:ss)
Launch	1	-1600	13:27:00
End second stage depletion burn	2	-46	13:52:54
PMG power on	3	0	13:53:40
Electrometer calibration (64 sec)	4	251	13:57:51
FEP start sequence	5	317	14:03:08
NEP start sequence	6	329	14:03:20
Start continuous current read (242 sec)	7	364	13:59:44
Begin FEP/tether deployment	8	400	14:00:20
End continuous current read	9	606	14:05:50
High current mode (44 sec)	10	607	14:05:51
First standard data frame (61 sec)	11	651	14:04:31
Day → night (spacecraft)	12	1170	14:13:10
Geographic equator (asc)	13	2147	14:29:28
Apogee (868 km)	14	2469	14:34:49
Magnetic equator cross (asc)	15	2545	14:36:05
High current mode (44 sec)	16	2853	14:41:13
High current mode (44 sec)	17	3194	14:46:54
Night → day (spacecraft)	18	3259	14:47:59
High current mode (44 sec)	19	3654	14:54:34
Geographic equator cross (dec)	20	5054	15:17:54
Perigee (194 km)	21	5314	15:22:14
Geomagnetic equator cross (des)	22	5416	15:23:56
Day → night (spacecraft)	23	6887	15:48:27
Geographic equator cross (asc)	24	7850	16:04:19
Apogee (868 km)	25	8190	16:10:10
Magnetic equator cross (asc)	26	8320	16:12:20
Night → day (spacecraft)	27	8970	16:23:10
High current mode (44 sec)	28	9031	16:24:11
High current mode (44 sec)	29	9313	16:28:53
Last electrometer data frame	30	9652	16:34:32
Electrometer calibration (33 sec)	31	9655	16:34:35
High current mode (through LOS)	32	9688	16:35:46
Geographic equator cross (dec)	33	10,761	16:53:39
Magnetic equator cross (dec)	35	11,158	16:59:16
Day → night (spacecraft)	34	12,600	17:23:36
Geographic equator cross (asc)	36	13,552	17:39:10
Magnetic equator cross (asc)	37	14,033	17:47:20
Loss of telemetry	38	14,415	17:54:33

The system was in a high current mode at this point, and no useful current telemetry are available to determine effects due to the change in cathode mode.

Figure 17 shows the altitude of the vehicle, and Figure 18 shows the orbital track. Note that perigee was in the middle of the day, so the day-night effect reinforces the altitude effects on local plasma density.

The PMG experiment was designed to measure currents and potentials across through the tether, as a function of tether voltage. Figure 19 shows a simplified schematic of the system. The load resistance could be set at 2.2 MΩ to make tether voltage measurements, and at 0, 100, 200, and 500Ω in current mode. The electrometer switched between 100 μA and 1 A full-scale modes for the corresponding measurements. The applied bias could be cycled from +65, +30, ±0, -65, -130 V. The ±0 modes correspond to zero bias, with diodes set for positive current flow in the signed directions. A "shorted" mode was available, but electrometer measurements in this mode were saturated, and are not shown.

The standard data frame sequence is illustrated in Figure 20. Each voltage, resistance sweep took approximately 10 seconds. The Bias voltages was varied at 10 second intervals, with the load resistance stepped at 2 second intervals. The 2 second dwell at 2.2 MΩ produces a potential measurement (LHS); subsequent measurements provide current at 500 Ω, 200 Ω, 100 Ω and 0 Ω load resistance. There is ~160 Ω resistance in the tether and PMG circuitry, besides the load resistance.

Note that no current flows at -0 V bias, due to the diodes in the circuit. Curves are labeled with the time tag obtained at the end of each 9 to 10 second sequence.(Timing varies slightly according to the measurements, because of an antiquated CPU in the control electronics).

In addition to the sequence of events illustrated here, there was sequence of the FEP hollow cathode every 10 seconds. Discharge power for the FEP was shut off for 10 seconds in every 90 seconds. Details of this effect will be discussed below.

IV. OBSERVATIONS

The great majority of the data collected by PMG are in the standard mode of bias voltage/load resistance sequences already illustrated. These data are examined in more detail below. First, however, the deployment sequence is shown.

A. DEPLOYMENT

The hollow cathodes were switched on prior to deployment. The assembly was released, and reached its 500-meter extension in a few seconds. This process was conducted with the +65V bias applied, and with zero load resistance.

Figure 21 shows the deployment data. The current drops sharply once the FEP separates from the Delta second stage. The initial sequence of variations is not clearly understood, but it is apparent that the system quickly settles down to ~0.075 A, with a modulation of ~5 to 10 mA. The large drops at 00:07:30 and 00:09:10 are due to the cycling of the FEP hollow cathode. The current effectively drops to zero. This behavior will be further explored below. For now, it should be noted that the system is still in daylight and at a relatively low altitude.

B. STANDARD MODES

The data from the basic mode were examined for the 2½ hour period during which such sequences were run. Subsequent to this, the "high current" mode was used, where the electrometer current

could not be measured. Figure 22 shows the data at the 01:32 mark, at perigee, just after crossing the magnetic equator.

These measurements show currents near the peak magnitude observed during the mission. The +65 V bias data show a potential measurement of ~125 V, implying a tether voltage of ~60 V. Subsequent bias steps show appropriate drops in potential. The +0V and +30 V bias show a variation due to the ~3s time constant of the bias circuit; the potential has not quite stabilized at the end of the potential measurement at those levels.

Variation around the behaviors shown here were driven by changing environments, and the cycling of the FEP hollow cathode power.

1. Tether current depends on the environment

The current through the tether depended strongly on the environment. Figure 23 shows one of first sequences. By contrast with the data shown in Figure 22, the currents observed for positive bias voltage are very low. In fact, they have fallen below the values observed five minutes earlier during the deployment. The current observed for -130 V bias is still relatively high, ~0.1 A. Figure 24 is a plot of data taken five minutes later (data frame 9) from 0:17:55 to 0:18:52. It is an example that indicates the current was at as low as 0.02 A (the electrometer resolution) for all bias voltages except -130 V. Most of the night-time data looked like this.

The peak currents were observed in daylight in the next orbit. Figure 25 and 26 show the data from frames 83 and 85. Figure 25 shows the most negative current measurement, ~ -0.3 A, taken at -130 V bias. Figure 26 shows the largest positive current,~0.18 A, taken at +65 V bias. The currents again dropped as the tether was eclipsed. In the final orbit, currents were just rising above zero as the sequencing ended.

Figure 27 shows the data from the last sequence, data frame 145. There is a modest positive current of ~0.05 A at +65 V bias, and a similar magnitude current observed at -130 V bias. The drop in the current observed at +65 V bias, 0 Ω load resistance occurs when the FEP hollow cathode shuts off, as addressed below.

The complete data set is summarized in Figures 28 and 29. The potential measurement from the 6 bias levels are shown in Figure 28. The top half of the figure shows, in descending order, data taken at +65,+30 and +0 bias. The bottom panel shows the data taken at -0, -65, and -130 V. The wide spread in the +30 and +0V data are due to the slow decay of the capacitor in the bias circuit, as shown above. The small gap at +100V is due to a bit error in the electrometer.

The non-zero values for the -0 V bias data are something of a mystery. The outlying data values are due to the FEP cathode cycle, as discussed below.

Figure 29 shows the currents measured at +65V bias, and -130 V bias, for zero load resistance. Note that the currents in the negative direction are uniformly larger in magnitude than the

positive currents, even though the net potential in that direction is less than the net potential for +65V bias. The downward spikes in the +65 V trace are again due to the FEP cycling.

C. THE EFFECTS OF HOLLOW CATHODE

As noted several times above, the operating condition of the FEP hollow cathode has dramatic effects on the system. It should be noted that when the FEP cathode discharge is shut off, gas continues to flow. The FEP cathode was programmed to cycle off for 10 seconds in every 90 seconds. The "ON","OFF" timing is shown in Table 2. The data were surveyed for evidence of the transitions, since no telemetry is available after deployment. In Table 2, the mark "X" means that there is no clear evidence of the HCA was under "ON" or "OFF" condition.

Table 2: Hollow cathode "ON","OFF" timing

"OFF"	"ON"	PERIOD
0:12:41	0:12:51	
0:14:01	0:14:11	90"
0:15:39	0:15:49	88"
0:17:13	0:17:23	84"
X	0:18:57	94"
X	X	
0:21:58	0:22:08	
X	X	
0:25:08	0:25:17	
X	0:26:50	93"
X	X	

X	X	
0:32:58	0:33:08	
X	X	
0:36:05	X	
X	0:37:50	
X	X	
0:40:47	0:40:57	
X	X	
0:43:54	0:44:04	
X	0:45:38	94"
X	X	
0:51:43	X	
X	0:54:58	
0:56:23	X	
X	X	
X	1:02:46	
1:05:43	1:05:53	
X	X	
1:14:57	1:15:07	
X	X	
1:18:02	1:18:11	
X	X	
1:21:06	X	
1:22:36	1:22:46	
1:24:11	1:24:21	95"
1:25:40	1:25:50	89"
1:27:12	1:27:22	92"
1:28:41	1:28:51	89"
1:30:12	1:30:22	91"
1:31:44	1:31:54	92"

1:33:14	1:33:24	90"
1:34:44	1:34:54	90"
1:36:14	1:36:24	90"
1:37:44	1:37:54	90"
1:39:15	1:39:25	91"
1:40:44	1:40:54	89"
1:42:13	1:42:23	89"
1:43:44	1:43:54	91"
1:45:13	1:45:23	89"
X	X	
1:48:12	1:48:22	
X	X	
1:51:13	1:51:23	
X	X	
1:54:13	1:54:23	
X	X	
1:57:11	1:57:20	
X	X	
2:00:11	2:00:21	
X	X	
2:03:11	2:03:21	
X	X	
2:06:11	2:06:21	
2:07:39	2:07:49	88"
2:09:09	2:09:19	90"
X	X	
2:12:07	X	
X	2:13:47	
2:15:06	X	
X	2:16:45	

2:18:07	X	
X	2:19:45	
X	X	
X	2:22:45	
X	X	
2:25:35	2:25:45	
X	X	
2:28:34	2:28:44	
X	X	
X	X	
X	X	
2:36:04	2:36:13	
X	X	
2:39:04	2:39:13	

The effects are studied by comparison of adjacent data frames. Figure 30 shows data from an "OFF" cycle at 1:25:39. The cathode shuts off while the bias is set at +65V, and the load resistance at 100 ohms. The current drops from 0.12 A abruptly to 0.03 A, with a further slow decrease to 0.02 A. Data from adjacent data frames are shown to demonstrate that environmental changes are not the cause. These measurements occur in the time period of peak tether current, and presumably the peak ambient electron density.

Figure 31 shows a second illustration, in a similar environment, but with a change of the opposite phase. Note that there is again a fairly large initial change, with a slower (one to two second time constant) approach to the full value.

The above two cases are for positive bias (generator mode). In the opposite polarity, almost no change is found. Figure 32 shows the data for an FEP off cycle at 01:39:15, and indicates a lack of variation at -130 V bias.

The change in plasma impedance indicated by these data affects the potential measurements, as well.

Figure 33 shows the contrast for HCA "ON" vs "OFF". When the HCA was on, the measured potential across the 2.2 MΩ load resistance was approximately 20 volts higher than when HCA was off. The system is now more obviously acting like a voltage divider. The potential drop across the plasma is ~15% of the total, indicating ~300 KΩ impedance in the plasma, when hollow cathode is off.

Figures 34 and 35 are other examples. The illustration in Figure 34 is nearly identical, and shows that the effect illustrated is not coincidental. In Figure 35 data taken at +0 V bias are shown. We can see that at 1:48:22 the potential rises sharply at the end. This is due to the hollow cathode turning on. The gradual slope is again due to the bias circuitry slowly decaying. Shifting the curve trace horizontally indicates a ~15 to 20 V drop in potential with the cathode off. Similar comparisons at -130 V showed no change.

D. SYSTEM IMPEDANCE

System impedance includes load resistance, tether resistance and the resistance of the plasma, In this case, we know the tether

system resistance (equal 160 Ω) and the load resistance. What we want to know is how the system impedance is influenced by plasma.

1. Plasma impedance

The impedance of the system can be estimated by dividing the measured voltage by the measured current. The known resistances can be subtracted off, the remainder should be due primarily to plasma effects. Figure 36 shows data from frame 80 with the inferred plasma impedance at different bias voltage and load resistance settings. We can see that the minus bias voltage always gives the lower plasma impedance. It seems that the plasma has negative resistance. The resistance declines as the current increases. Data from data frame 91 are show in Figure 37. Here the HCA is off during the +65 V measurements giving substantially higher impedance estimates. The impedance is not as high as the ~300 KΩ obtained above at low current (2.2 MΩ), however. It is apparent that the impedance depends strongly on the bias voltage and load resistance, implying a dependence on current.

The data are show as a plot of impedance vs current in Figure 38 (from data frame 80). The larger magnitude currents give lower impedance, and negative currents show lower impedance than positive current of the same magnitude. This effect depends on the environment, also. Figure 39 shows data taken earlier, at 00:18:05. The impedance never drops below 1 KΩ, and exceeds 10 KΩ. It is a strong evidence that the system impedance depends on the plasma density.

V. SUMMARY AND CONCLUSIONS

During the PMG experiment, the flight telemetry system transmitted 146 frames of electrometer current measurements. Each frame consisted of all combinations of 6 bias voltages and 5 load resistances to characterize the electrical connection to the surrounding LEO plasma.

Reviewing, the following facts were observed.

1. The highest current measured in Generator mode is approximately 0.18 A.
2. The highest current measured in Motor mode is approximately 0.30 A.
3. The highest induced potential in Generator mode is approximately 120 V.
4. The FEP-HCA off state gives almost zero current in Generator mode. It has no effect in motor mode.
5, Almost no current is observed at night.
6. It is not effective for tether system be used as generator or motor in night. The ionosphere will not supply enough electrons for the power.
7. According to the experiment, the currents depend on HCA working state. The HCA effectively decreases the impedance between plasma and the satellite.

The current may not be proportional to the induced potential. The limitation seems to be how many electrons can be supplied by the ionosphere.

In this experiment, the tether only deployed 500 meter. It is not known how a longer tether will affect the system efficiency. We will expect further experiment.

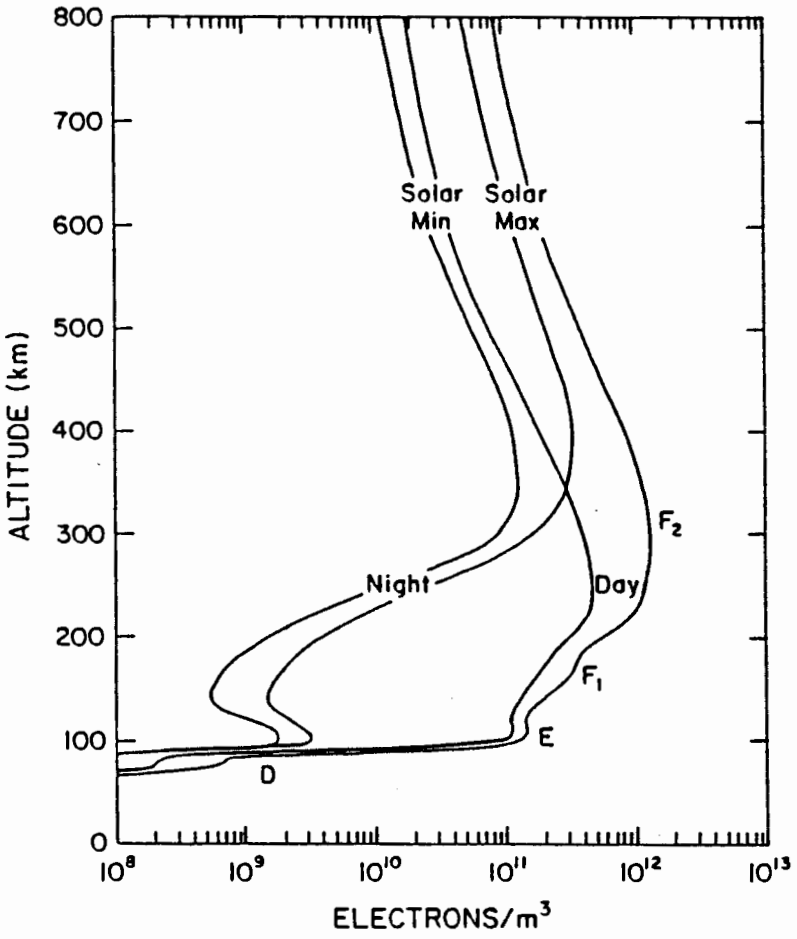

Figure 1: Plasma density with altitude in the ionosphere

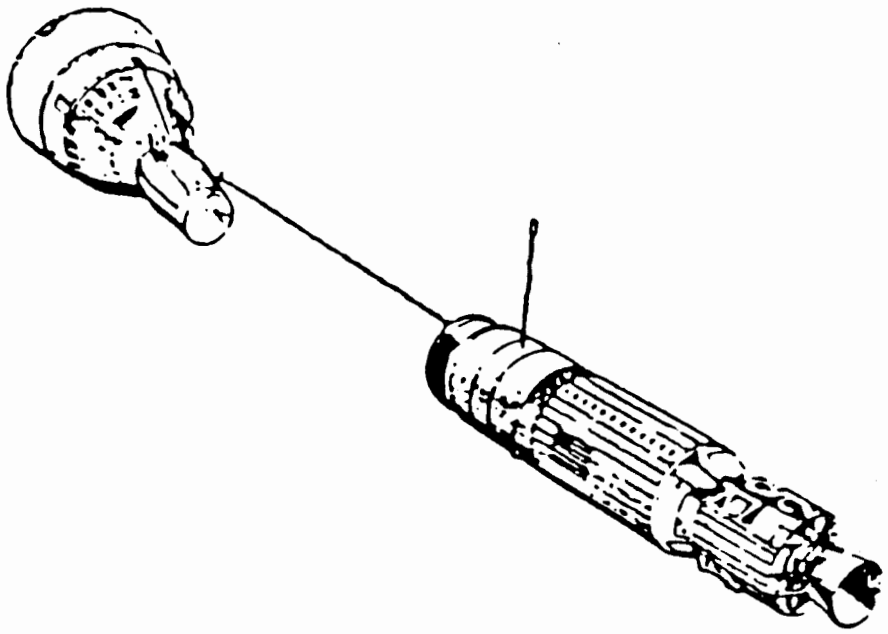

Figure 2: Gemini spacecraft tethered configuration

TYPICAL ELECTRODYNAMICS MISSION SCENARIO

1. ORBITER ATTAINS APPROXIMATELY CIRCULAR 160 NMI (296 KM) ORBIT.
2. UNLATCH SATELLITE AND DEPLOY OUTWARD USING THE 12 METER DEPLOYMENT BOOM.
3. RELEASE SATELLITE AND CONTROL UPWARD TRAJECTORY USING TETHER REEL MOTOR 20 KM DEPLOYMENT (WITH TWO 1.5 HOUR STOPS AT 10 KM AND 15 KM) REQUIRES APPROXIMATELY 9.2 HOURS.
4. SATELLITE CONTROLLED ON-STATION 20 HOURS.
5. RETRIEVE SATELLITE, (REQUIRES APPROXIMATELY 3.8 HOURS) DOCK TO BOOM TIP, RETRACT BOOM AND LATCH DOWN SATELLITE.

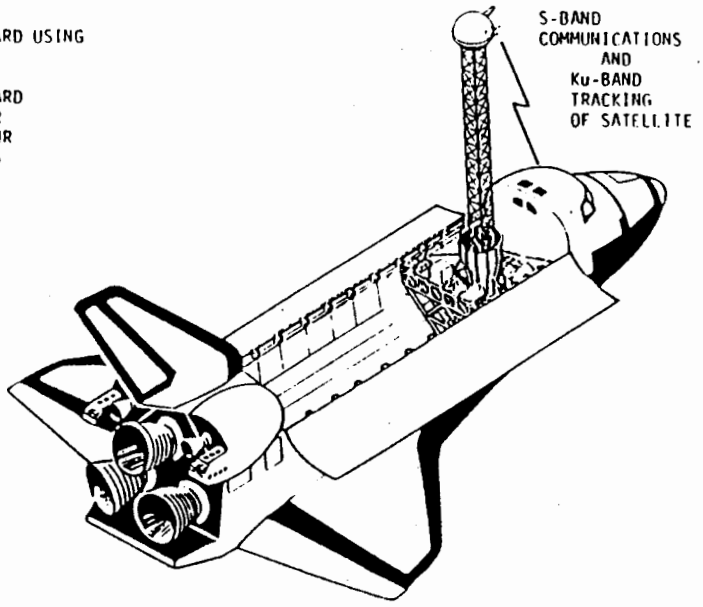

Figure 3: TSS operation concept

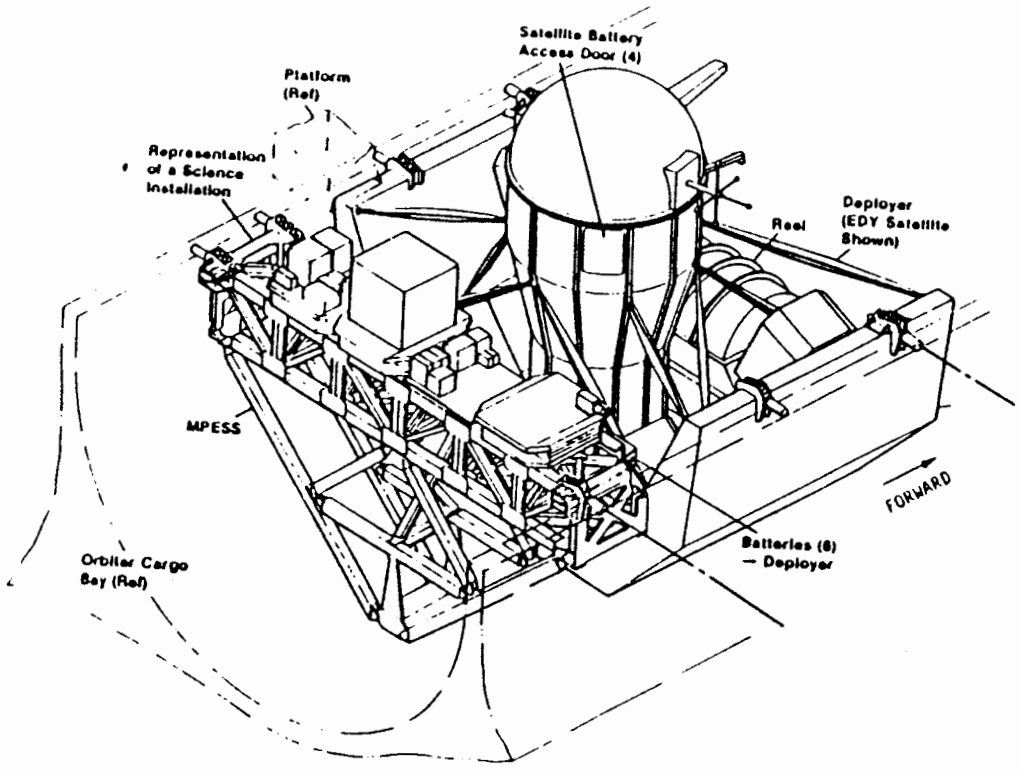

Figure 4: TSS configuration in cargo bay

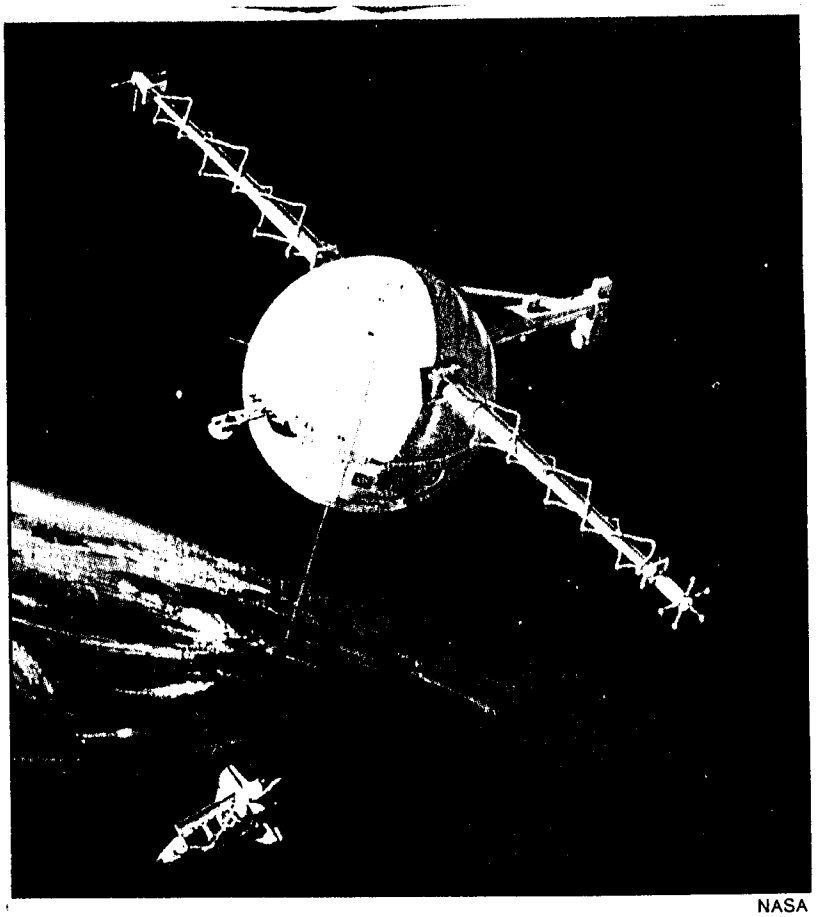

NASA

Astronauts will reel out an 1,140-pound spherical satellite 12.4 miles above the shuttle on a tether no bigger than a bootlace.

Figure 5: Shuttle-tether-satellite sketch

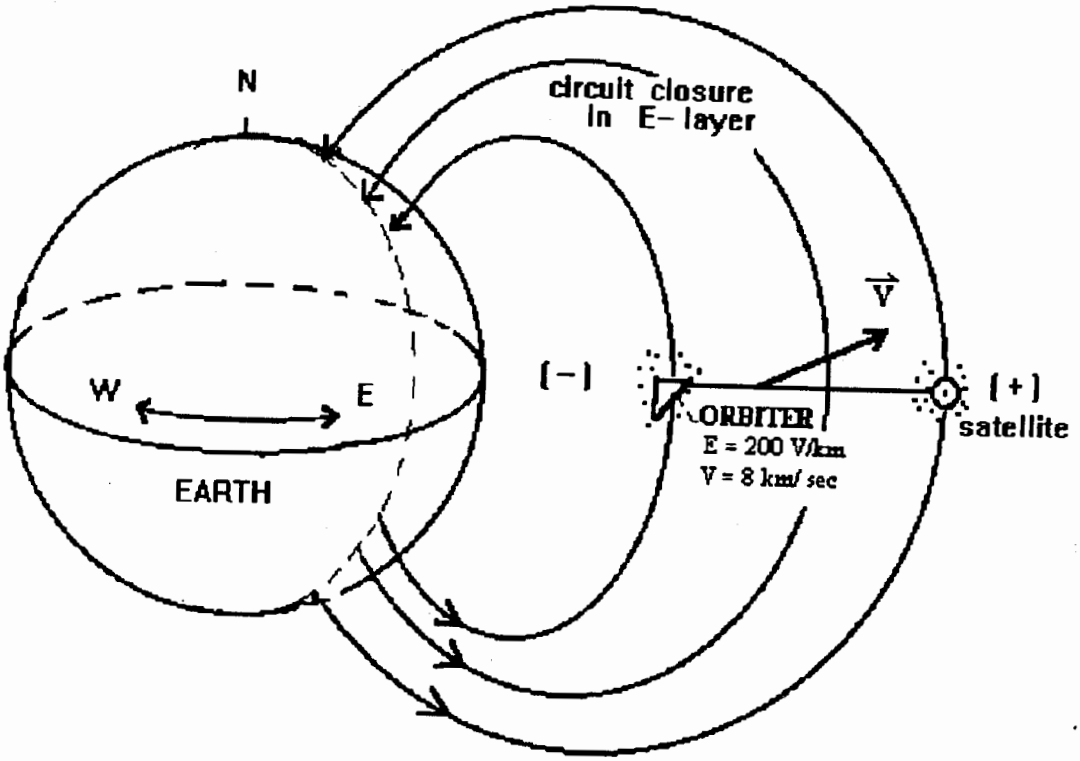

Figure 6: TSS around Earth's ionosphere as moving conductor

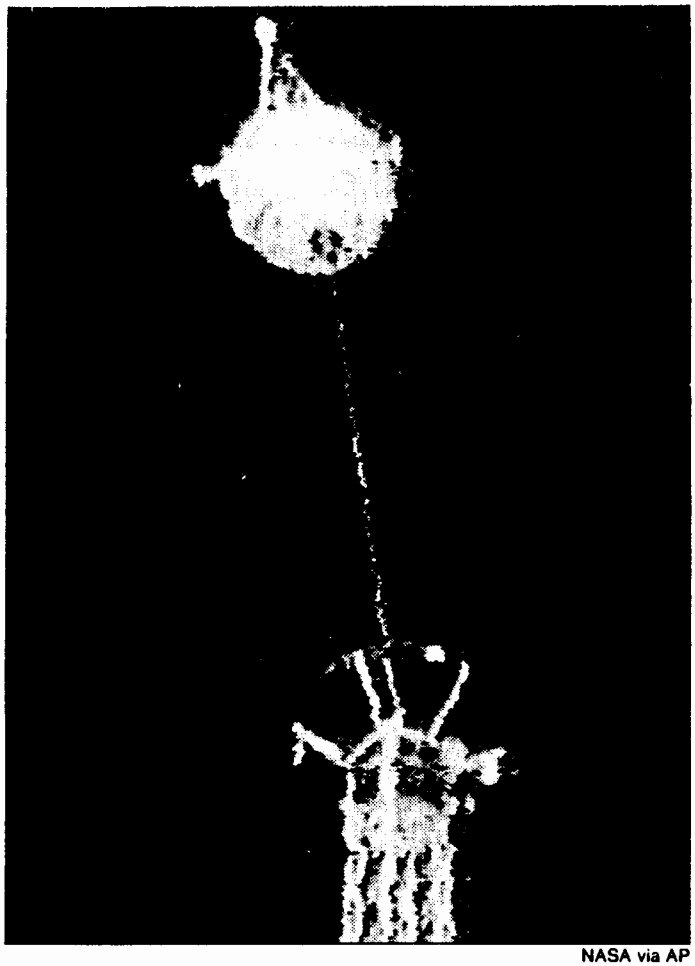

NASA via AP

RELEASE: A tethered satellite moves away from its shuttle cradle Tuesday. Atlantis was over the Pacific just off Chile's coast.

Figure 7: TSS-1, deployed satellite

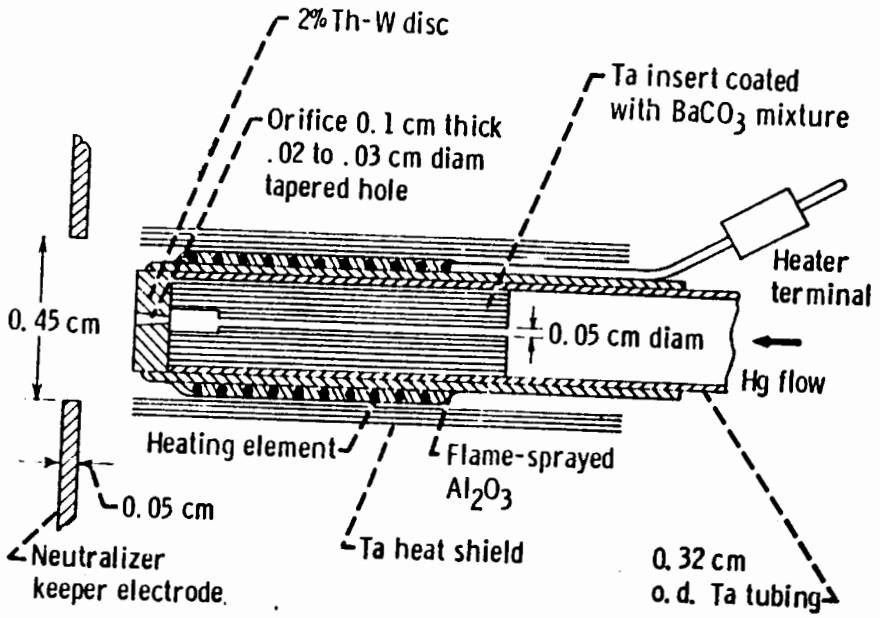

Figure 8: Plasma-bridge neutralizer cathode

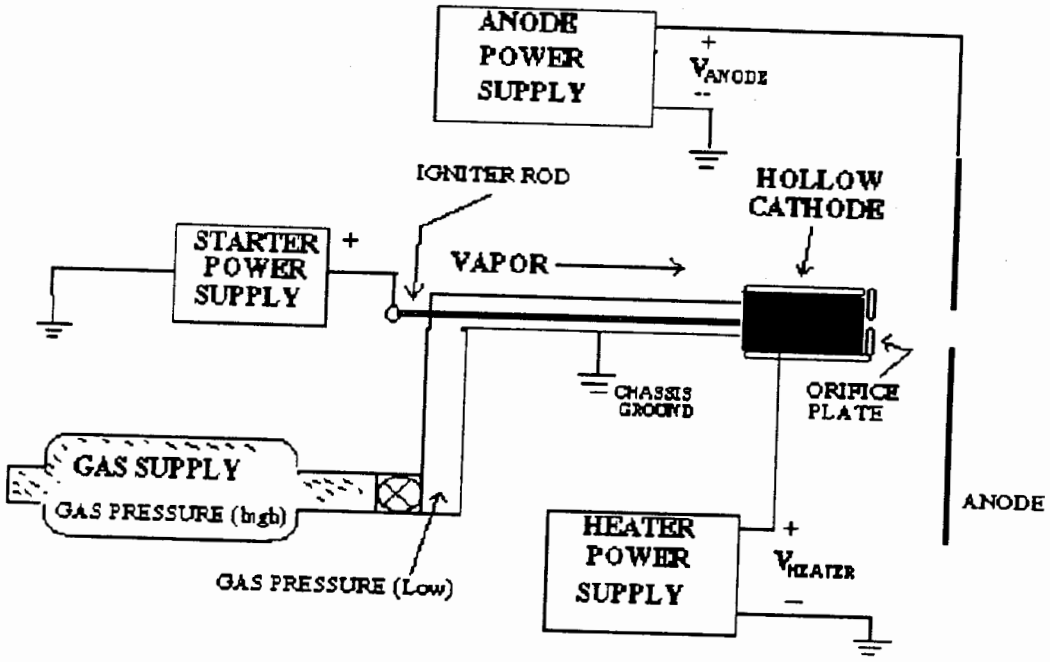

Figure 9: Hollow Cathode Assembly configuration

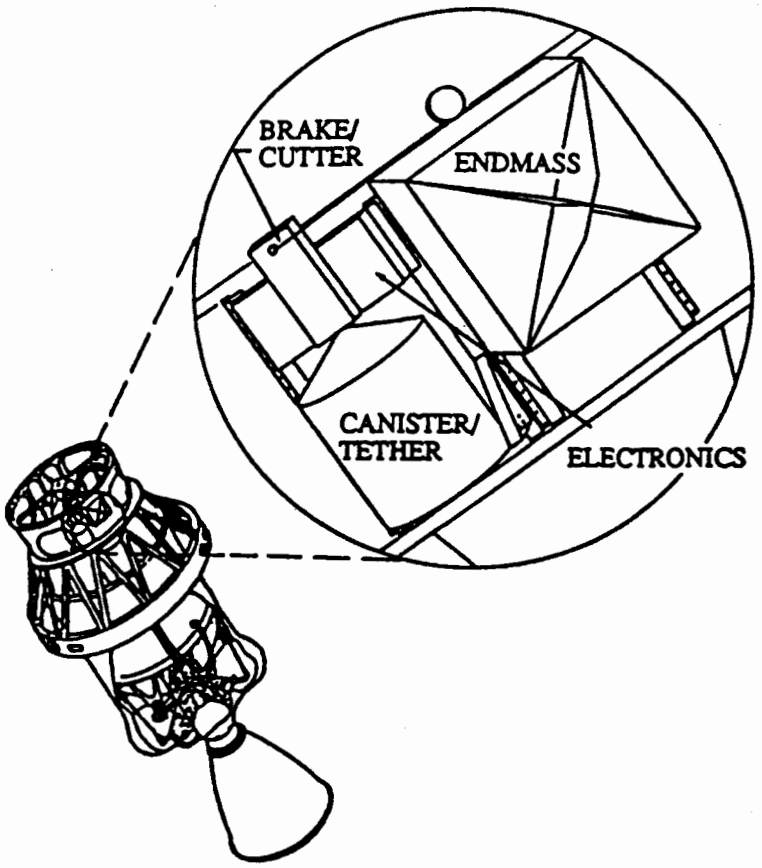

Figure 10: SEDS arrangement inside Delta II second stage

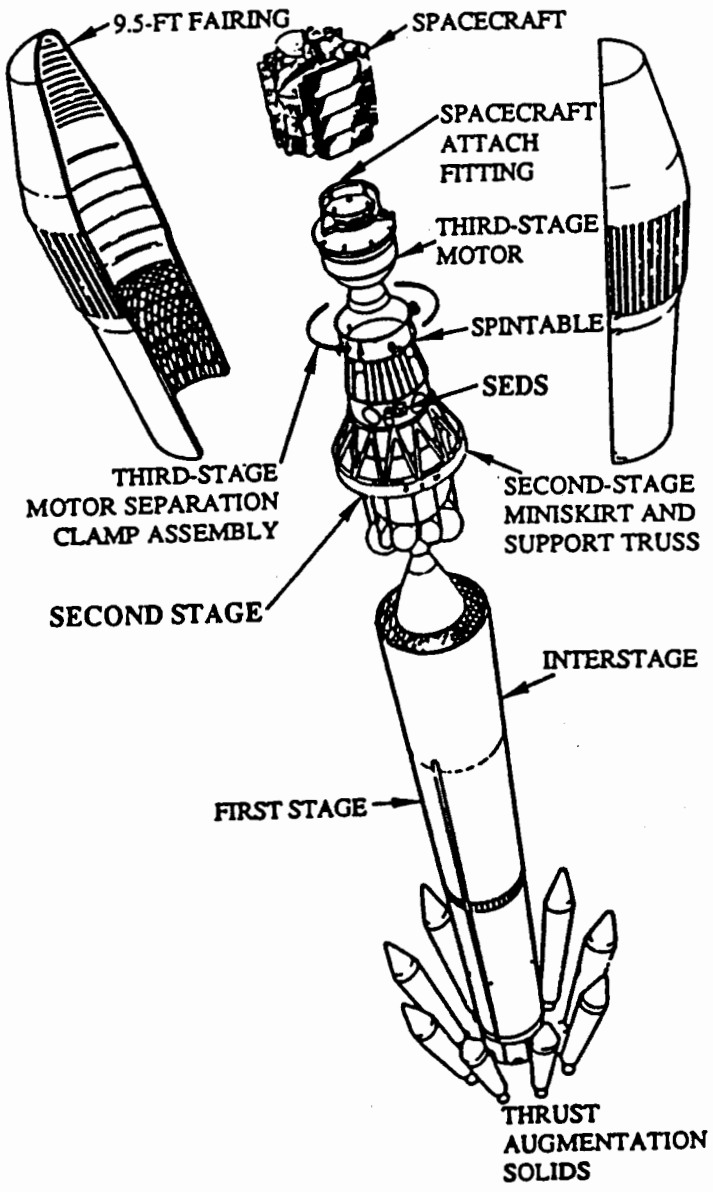

Figure 11: SEDS location on Delta II launch vehicle

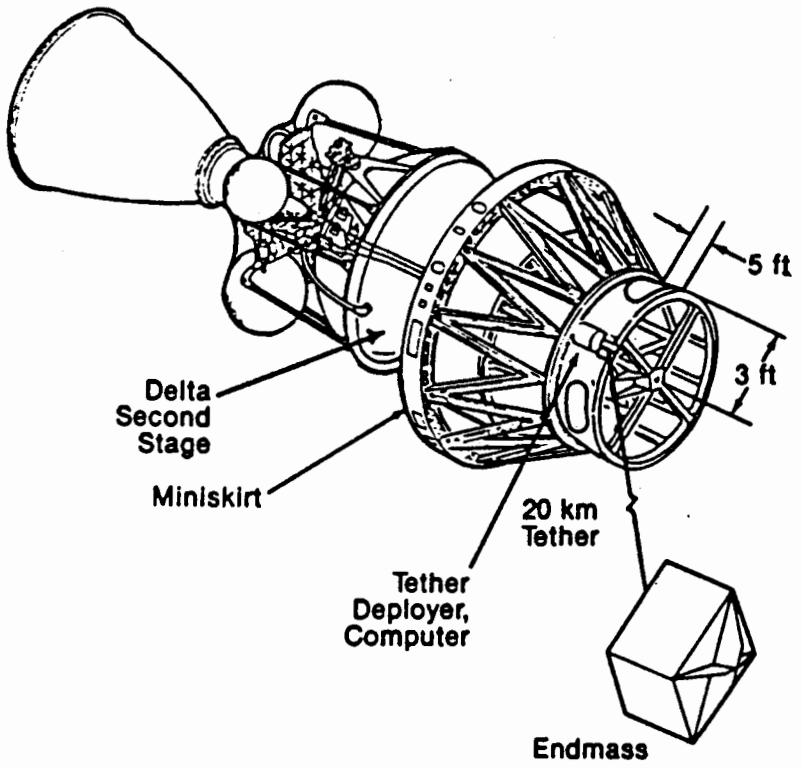

Figure 12: Delta second stage with deployed tether

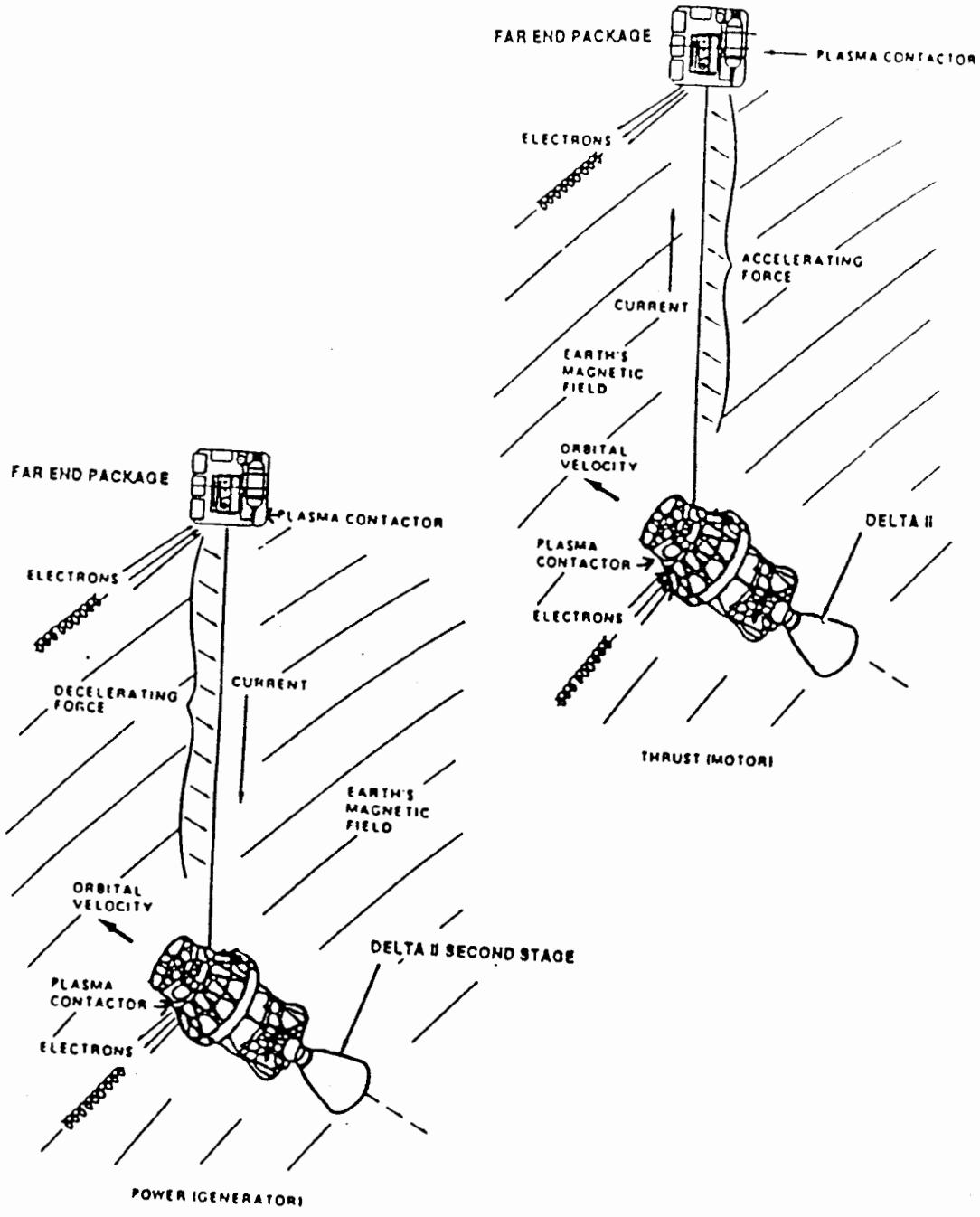

Figure 13: PMG demonstration of electrodynamic tether principles

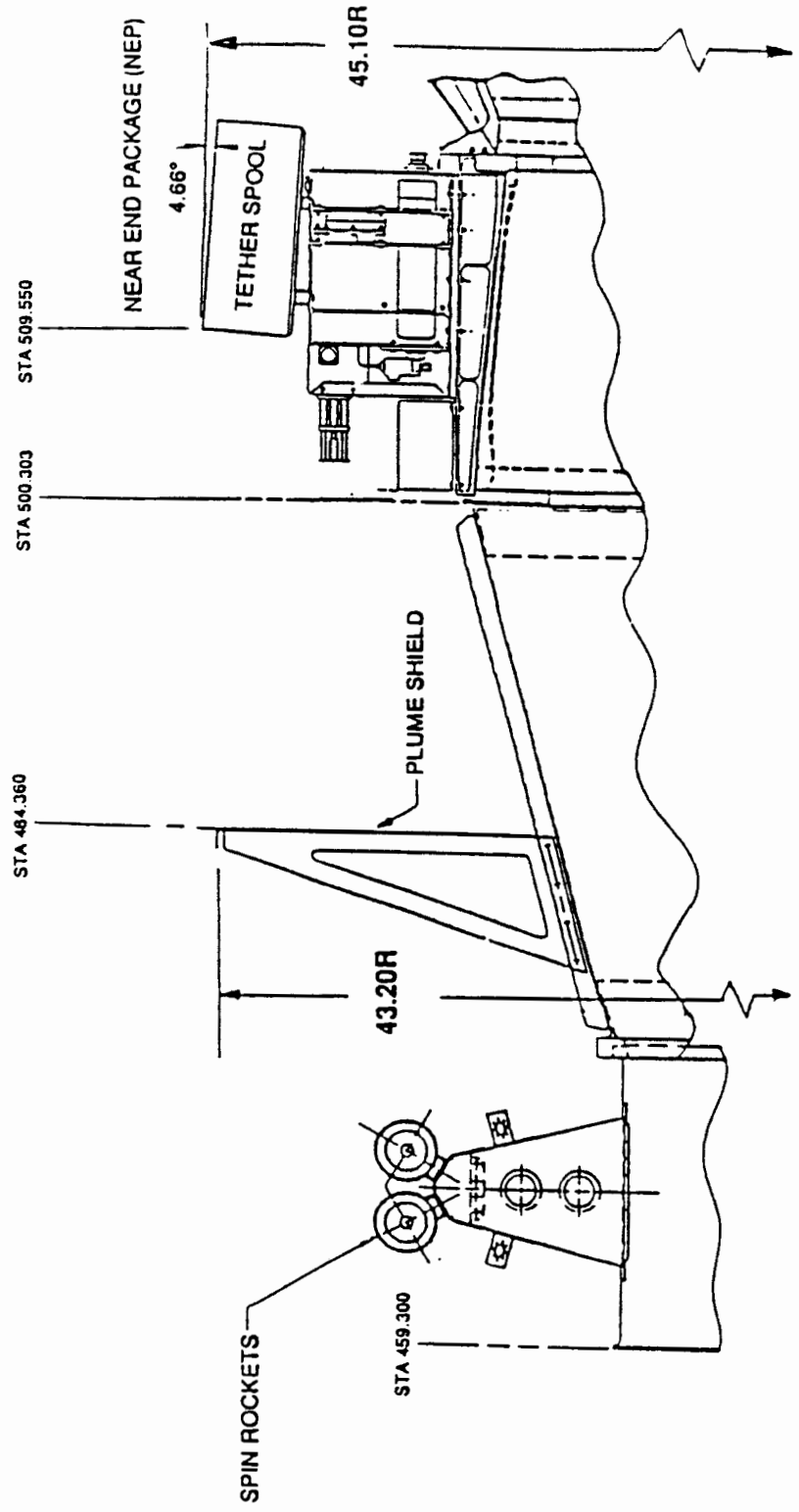

Figure 14: Location of PMG package on Delta second stage

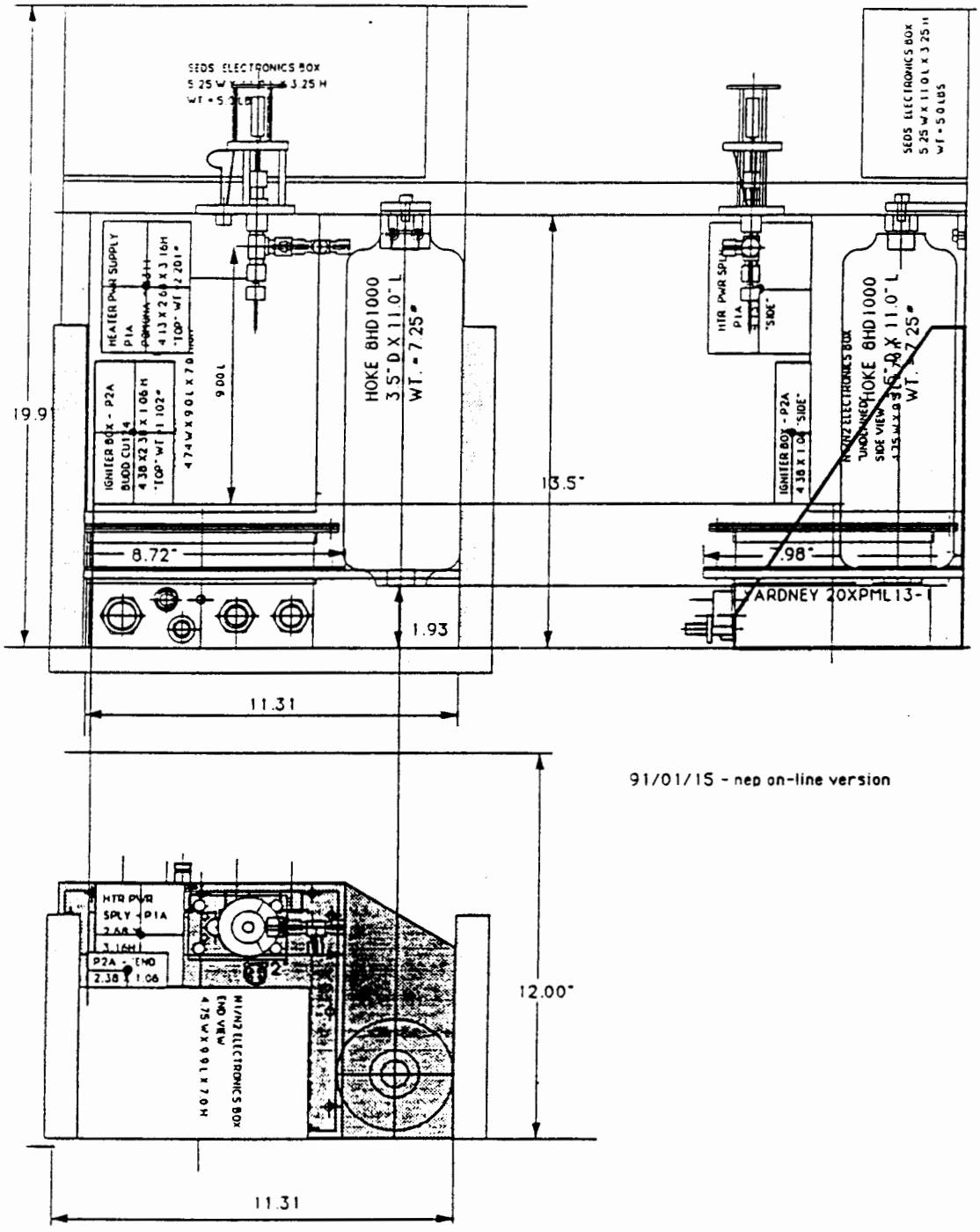

Figure 15: PMG mechanical layout

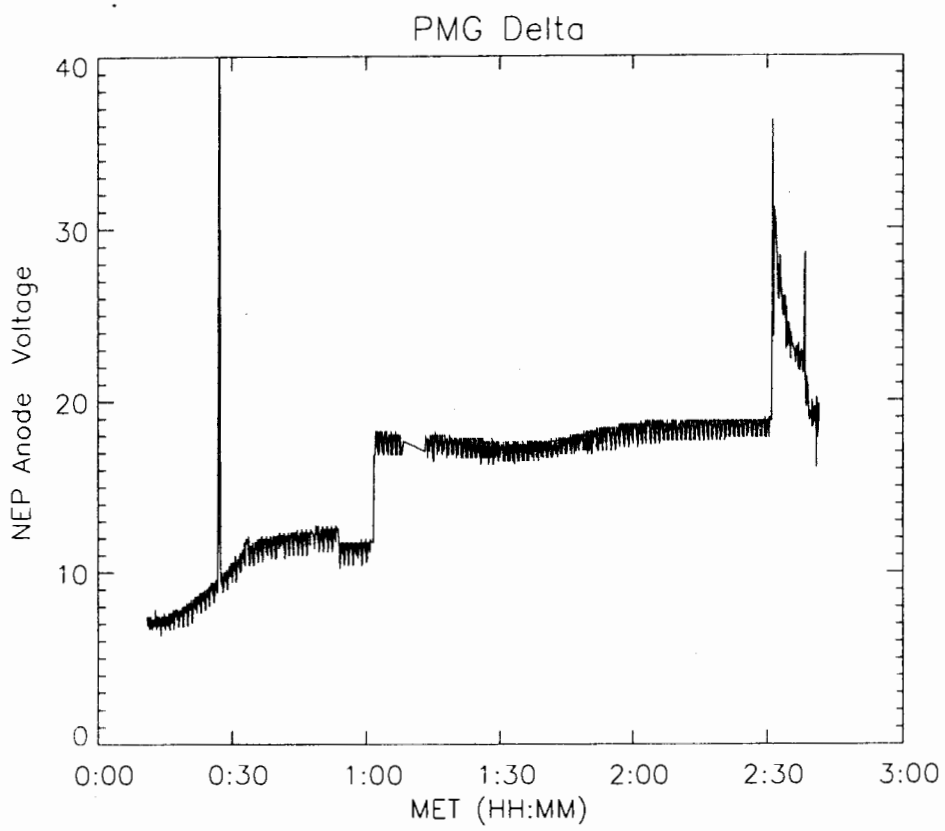

Figure 16: NEP anode voltage with timing

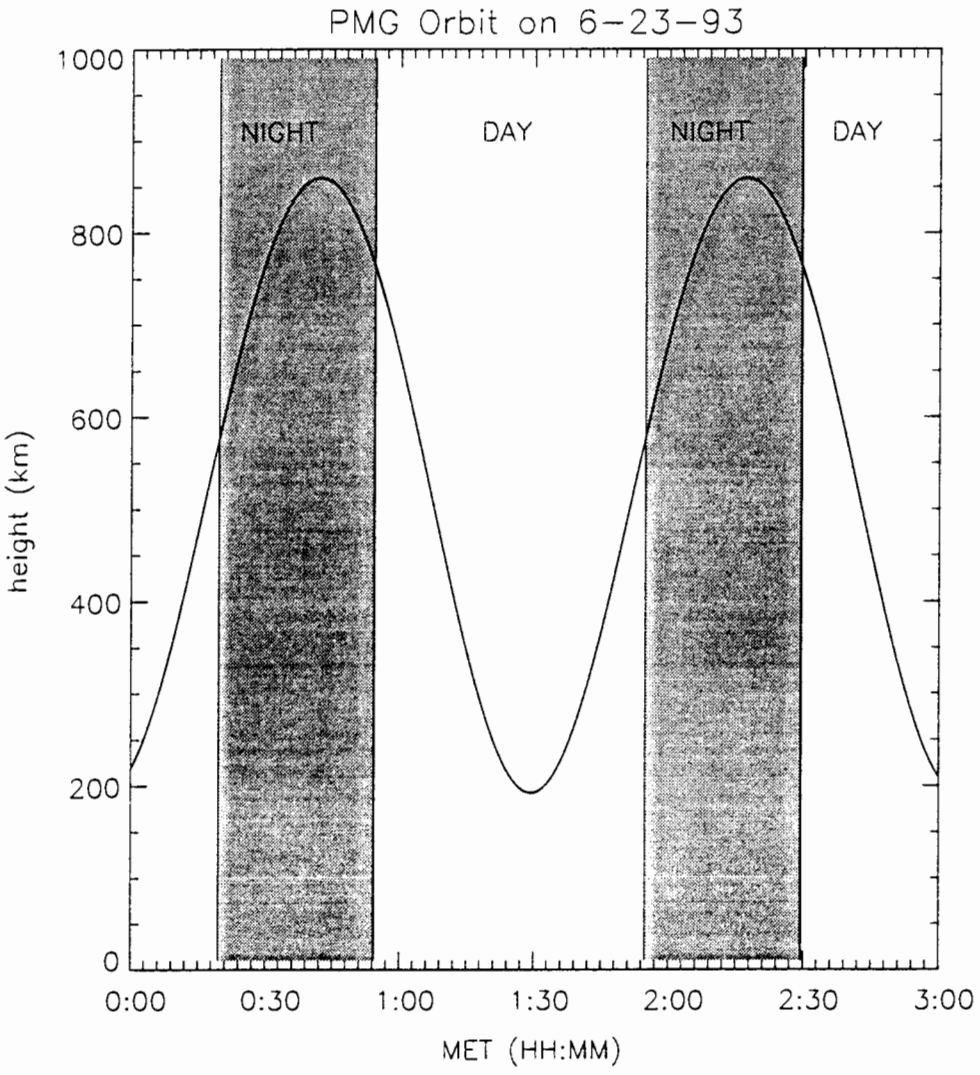

Figure 17: Altitude of orbiter

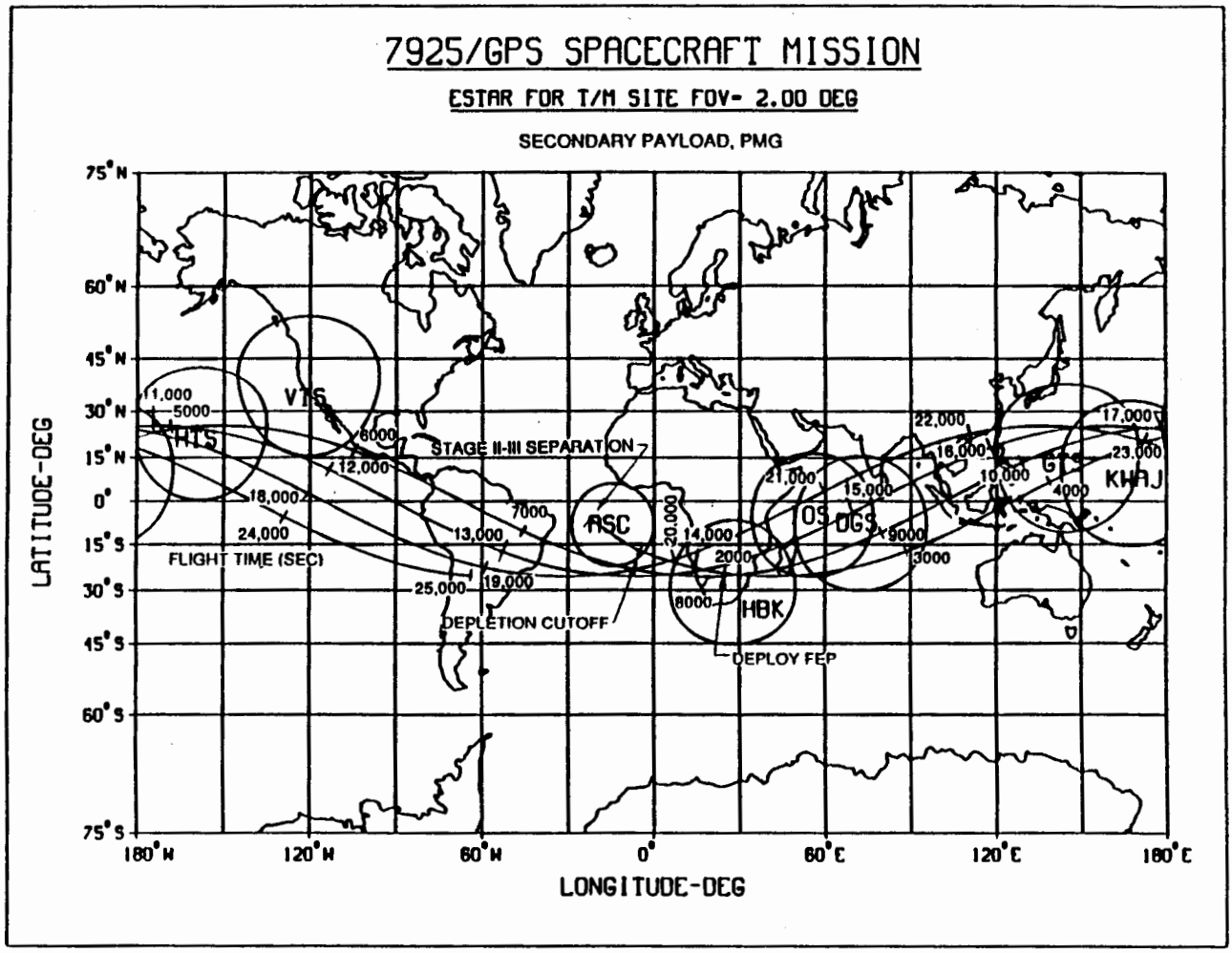

Figure 18: Orbiter track diagram

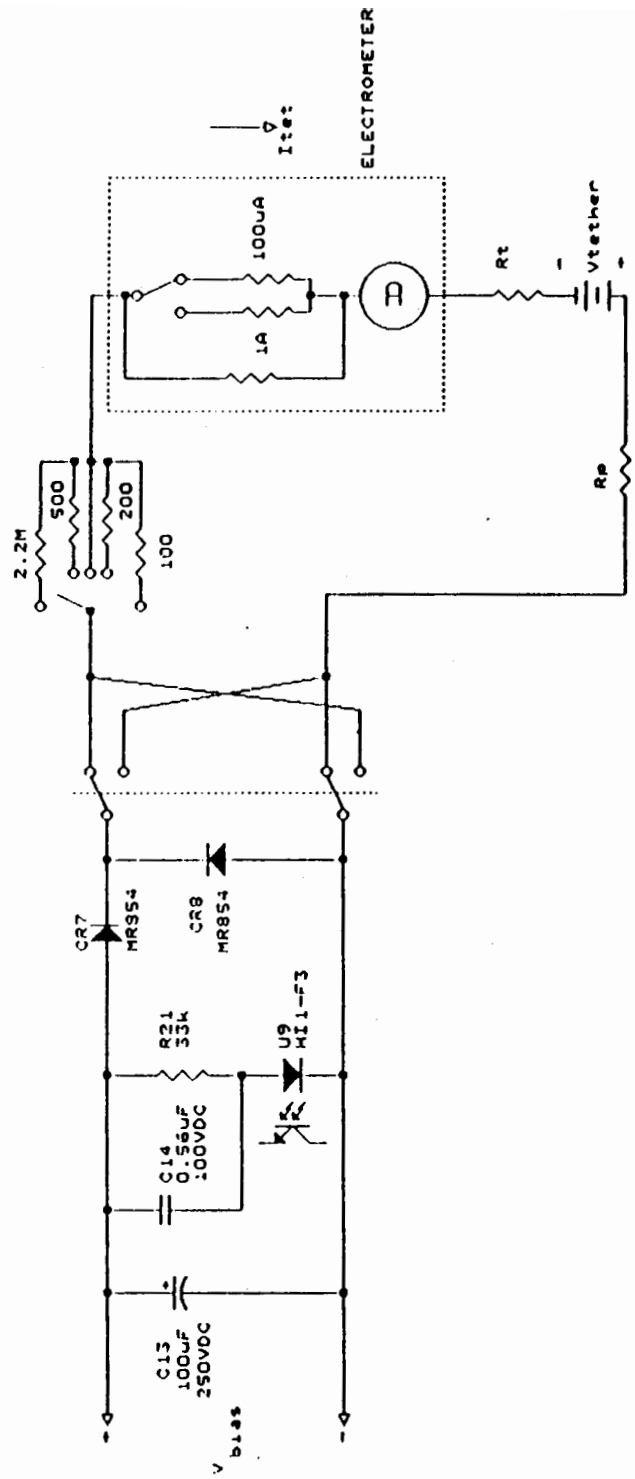

Figure 19: PMG circuit diagram

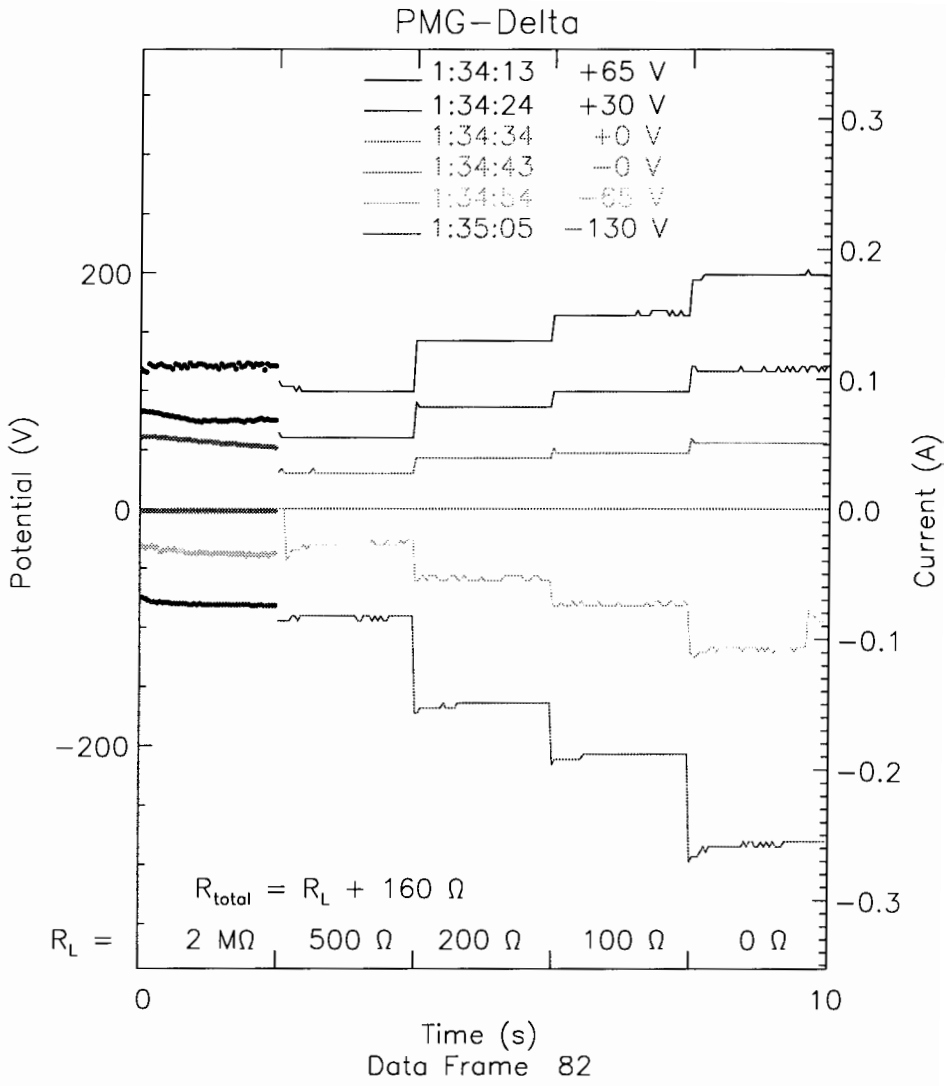

Figure 20: Standard data frame sequence

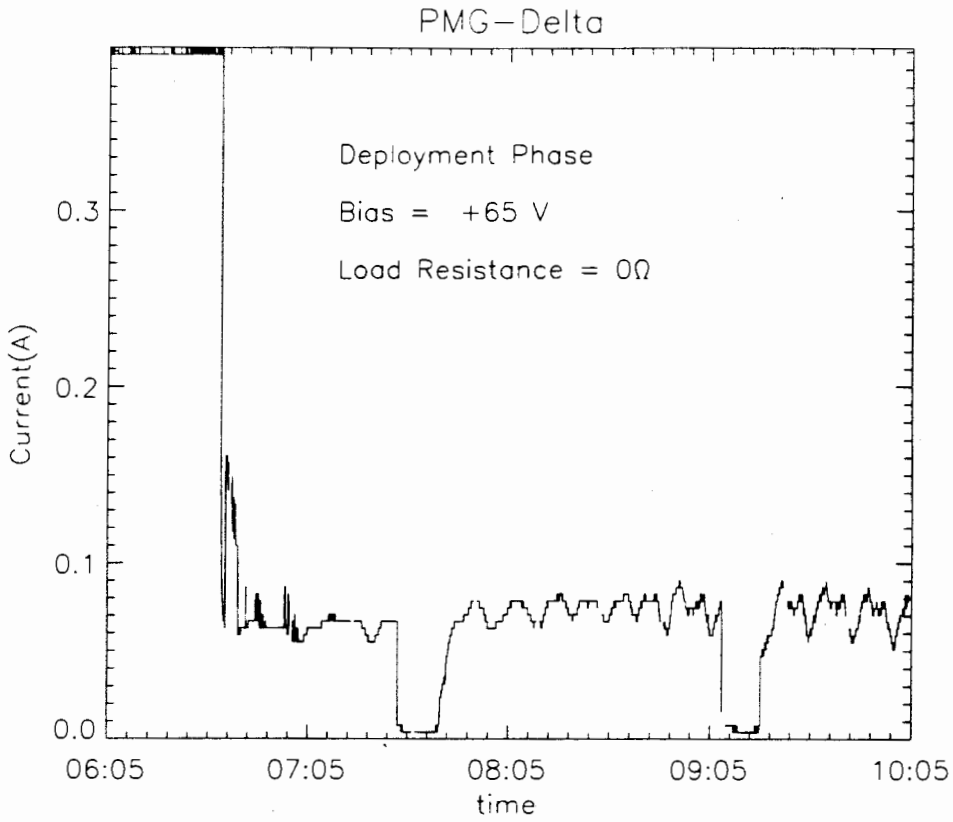

Figure 21: PMG-Delta deployment phase

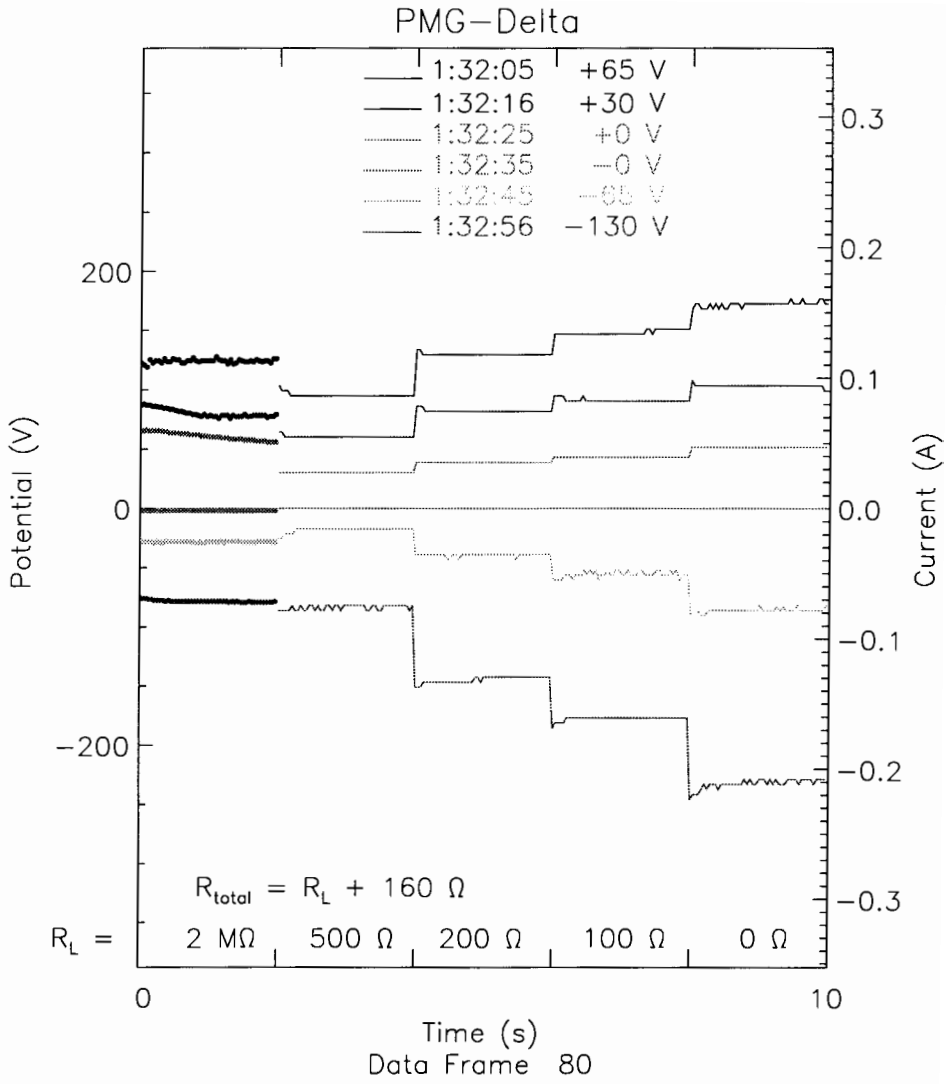

Figure 22: Data frame 80

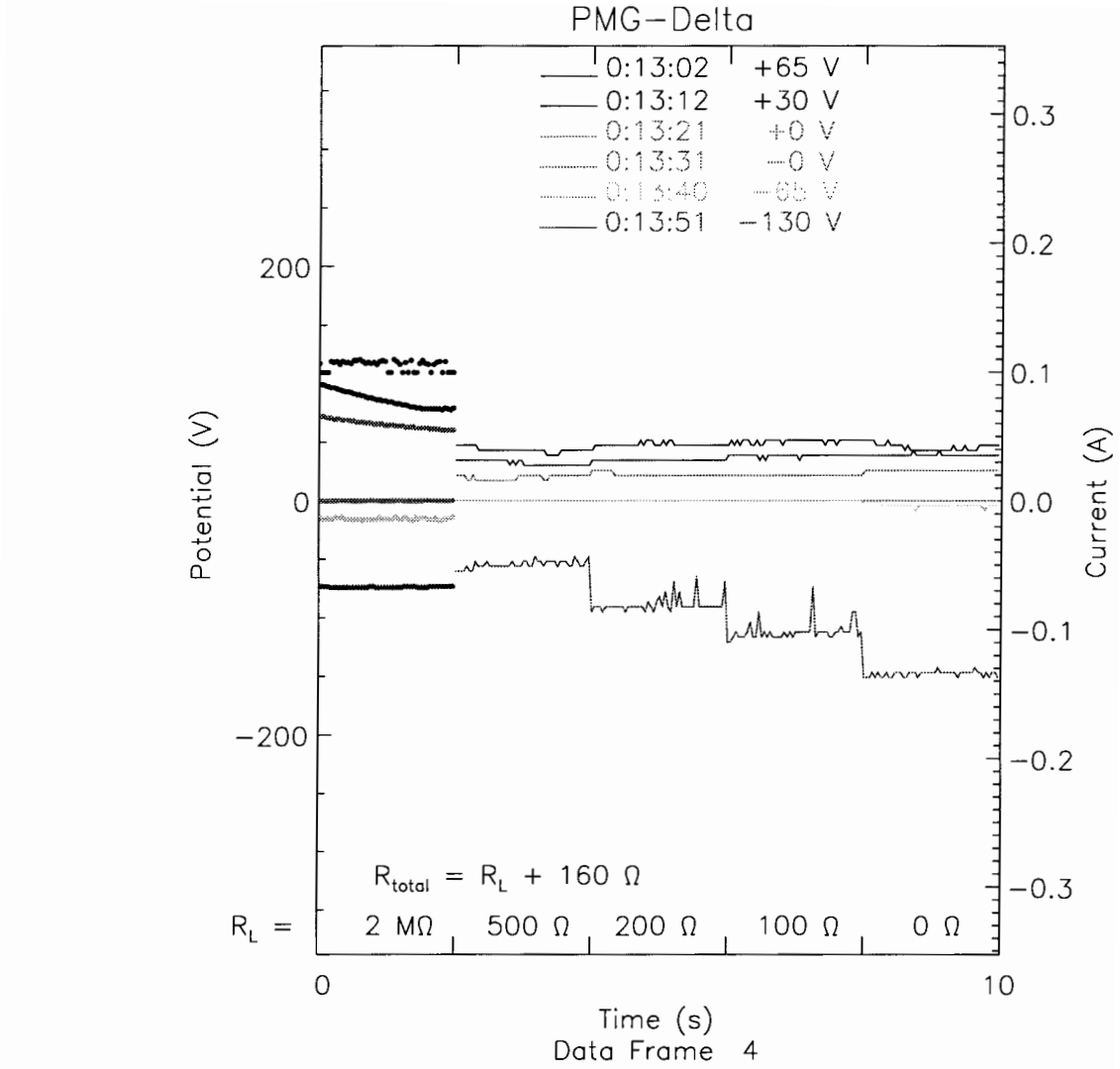

Figure 23: Data frame 4

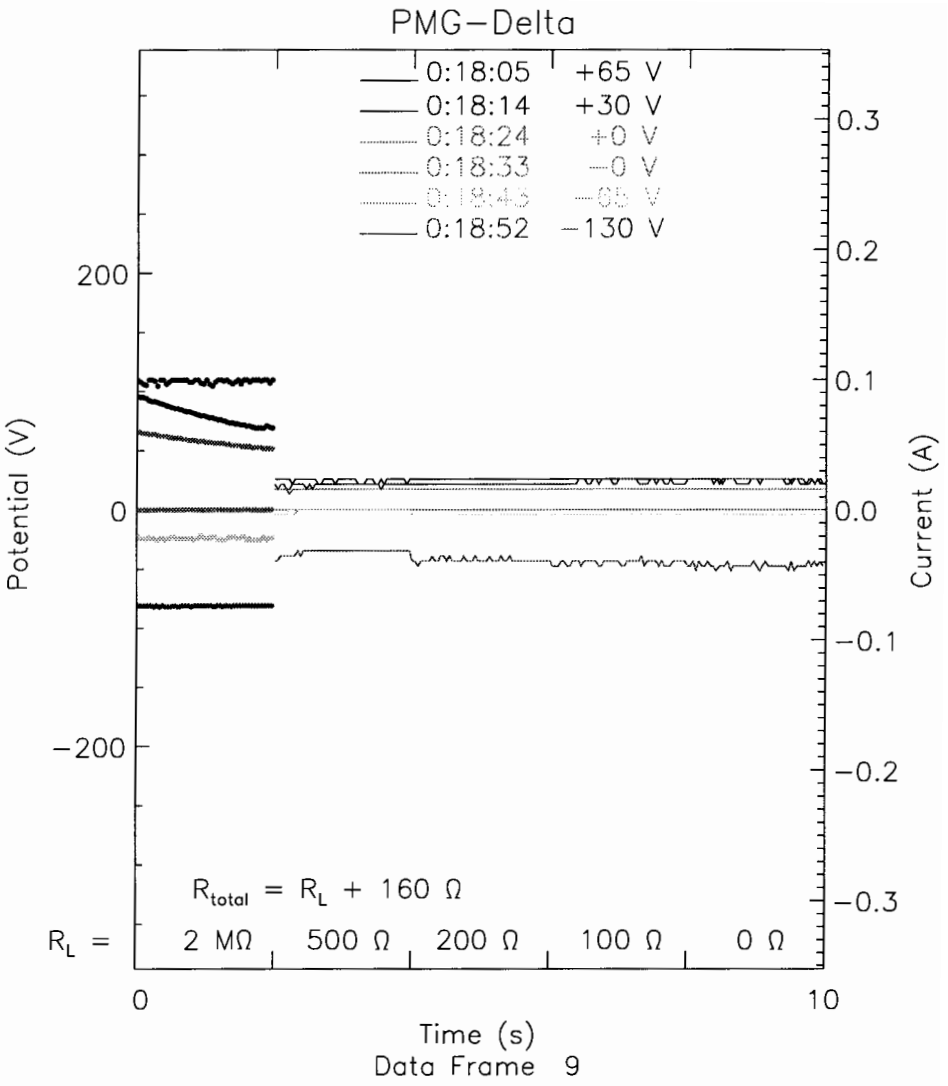

Figure 24: Data frame 9

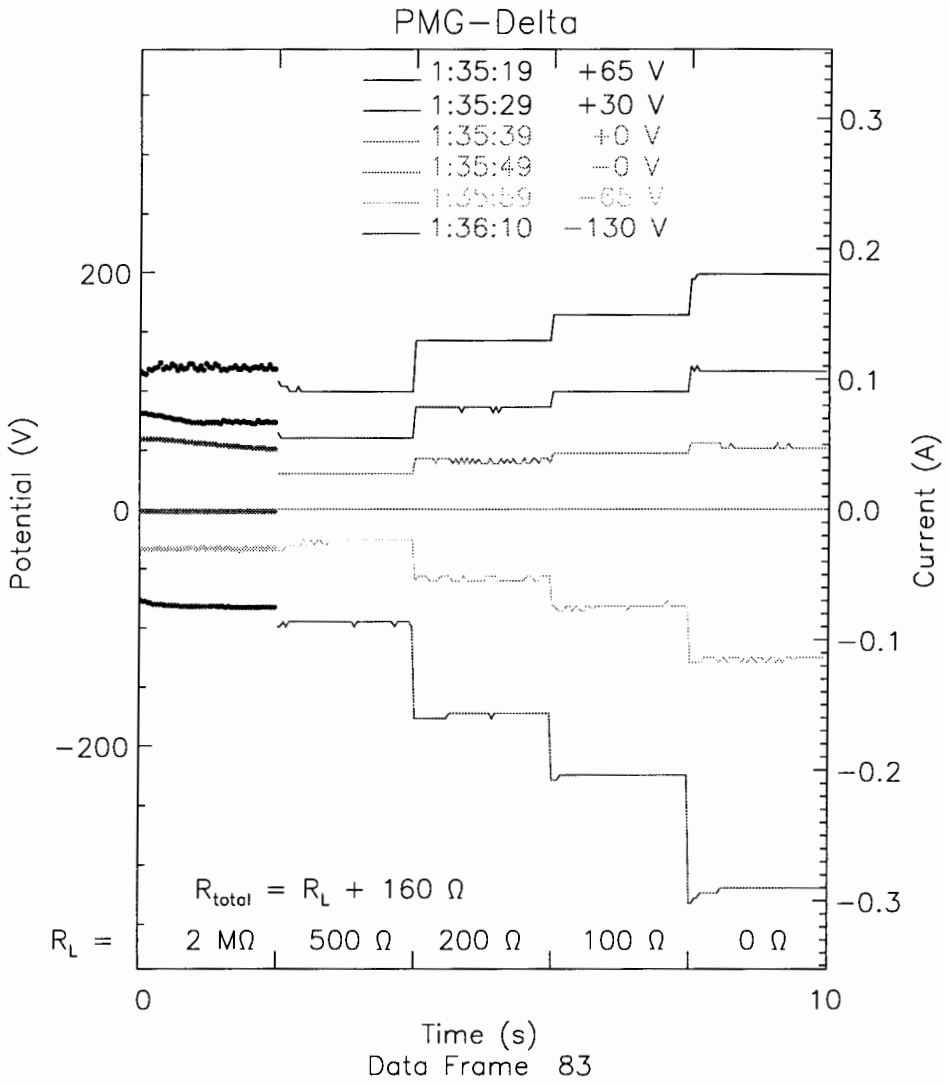

Figure 25: Data frame 83

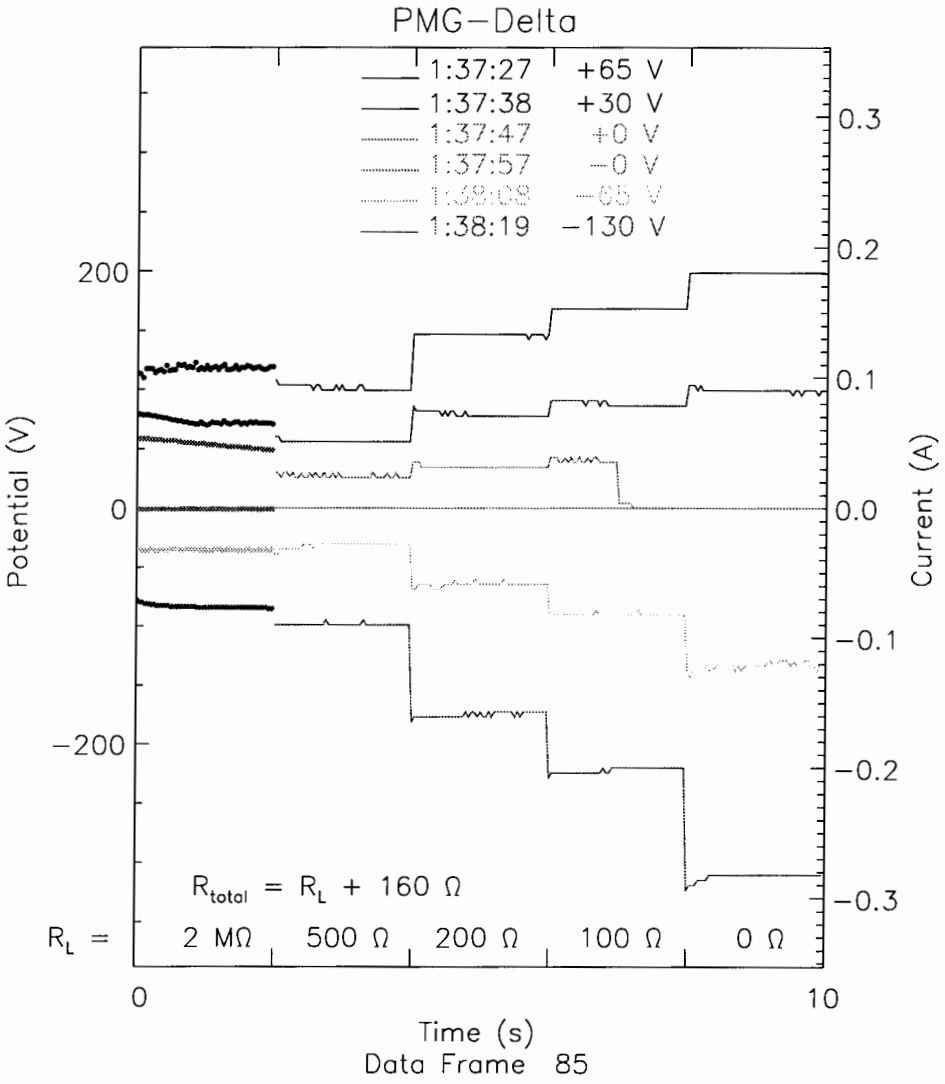

Figure 26: Data frame 85

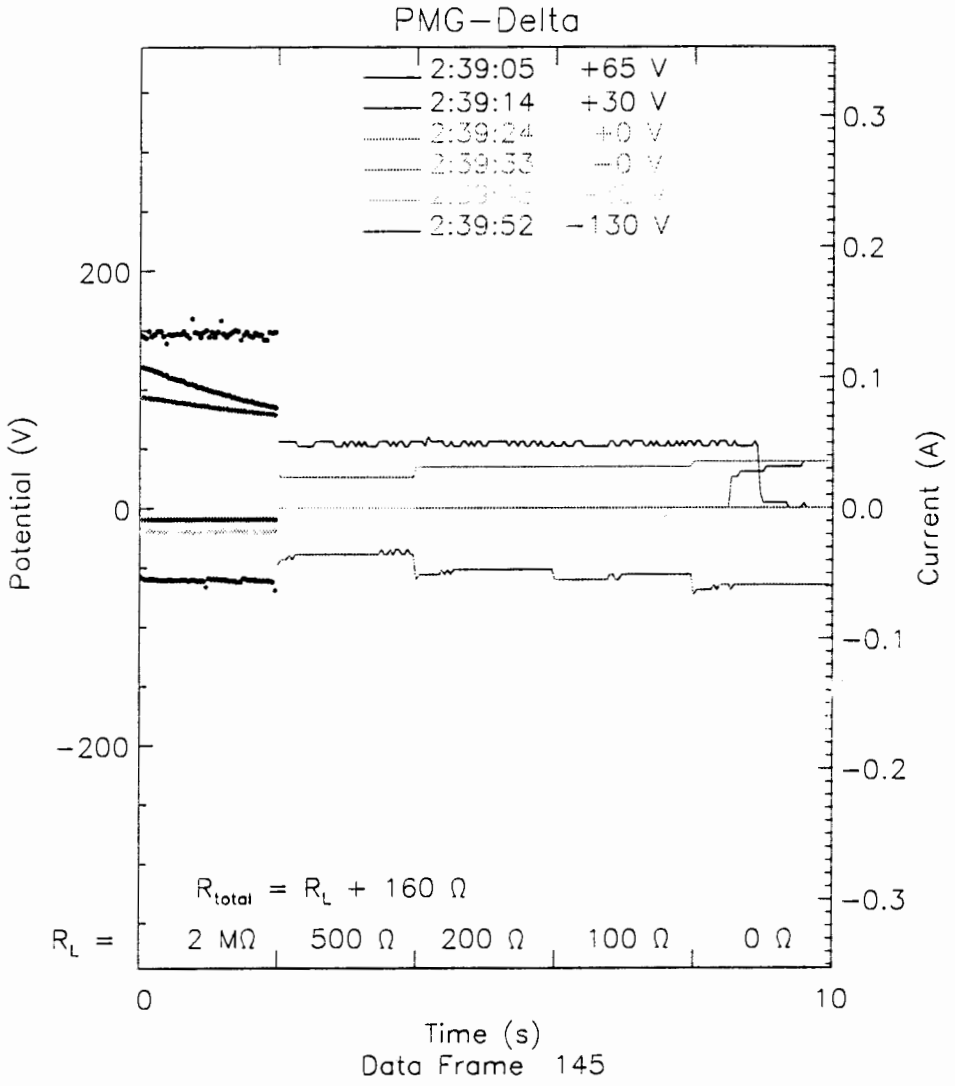

Figure 27: Data frame 145

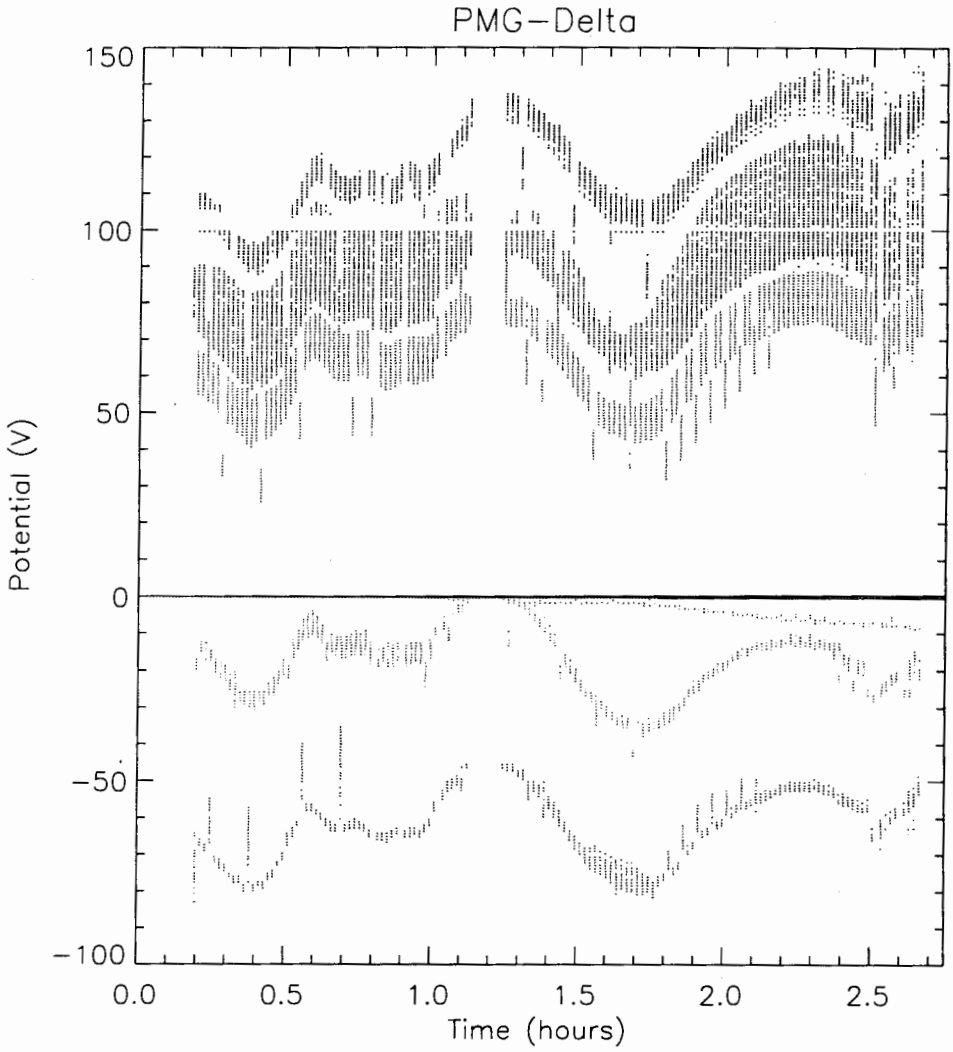

Figure 28: Potential summary

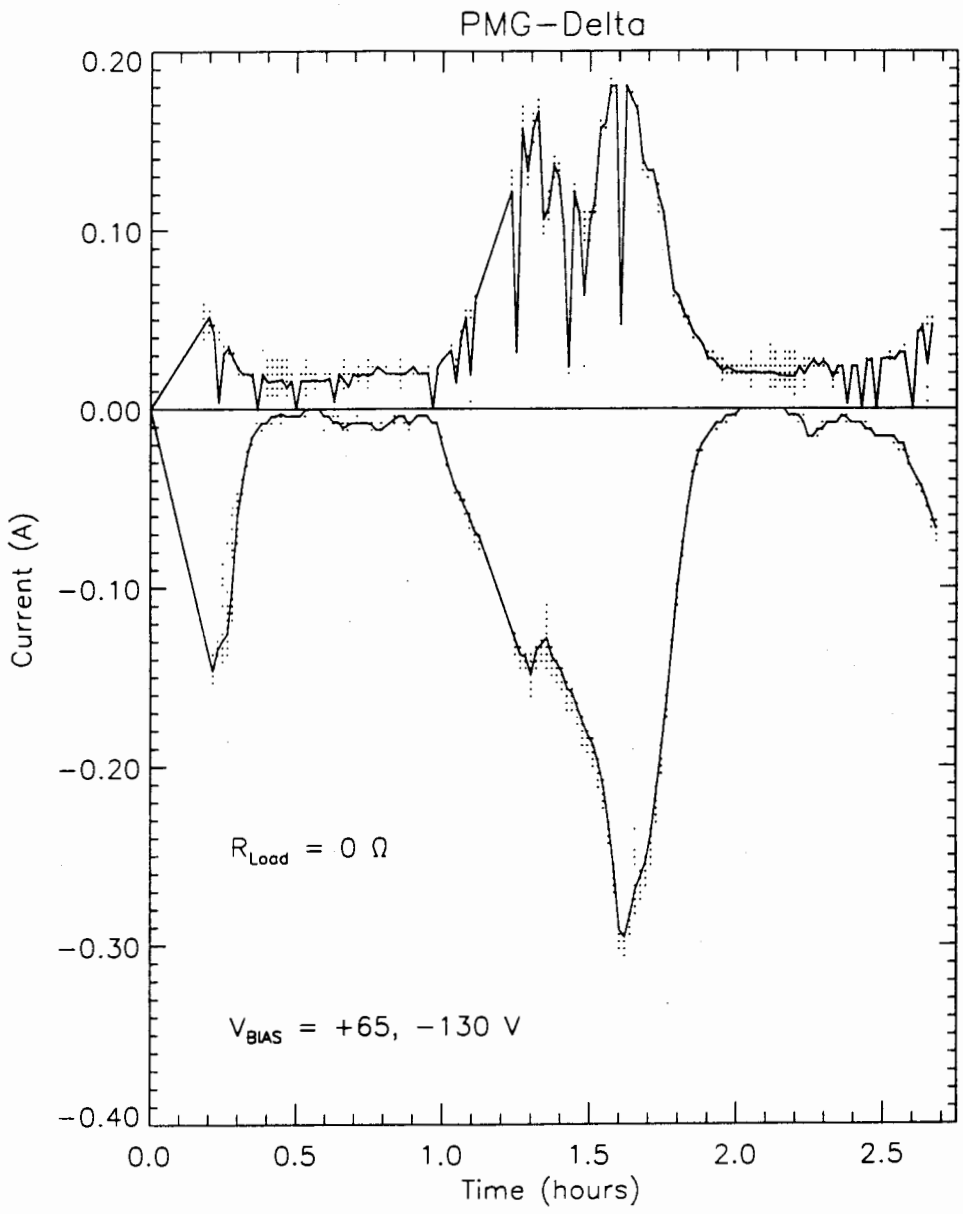

Figure 29: Current summary

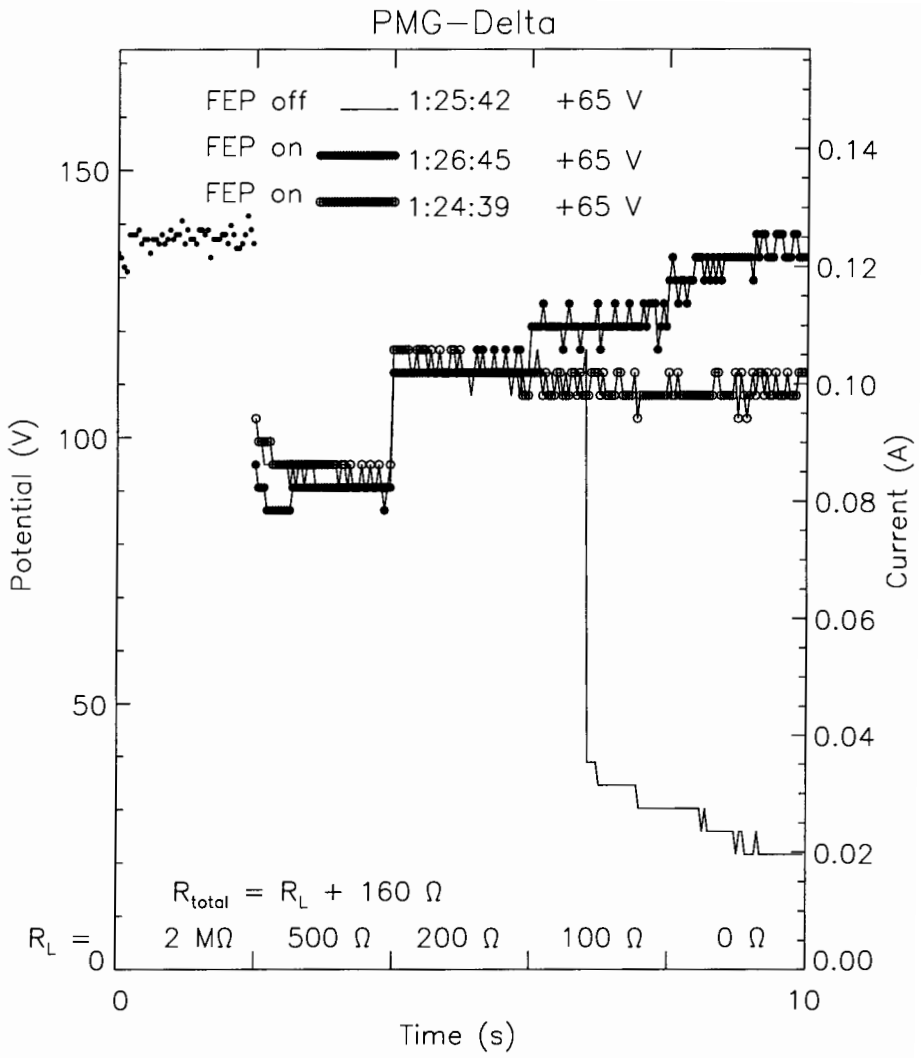

Figure 30: Current change with FEP/HCA working state

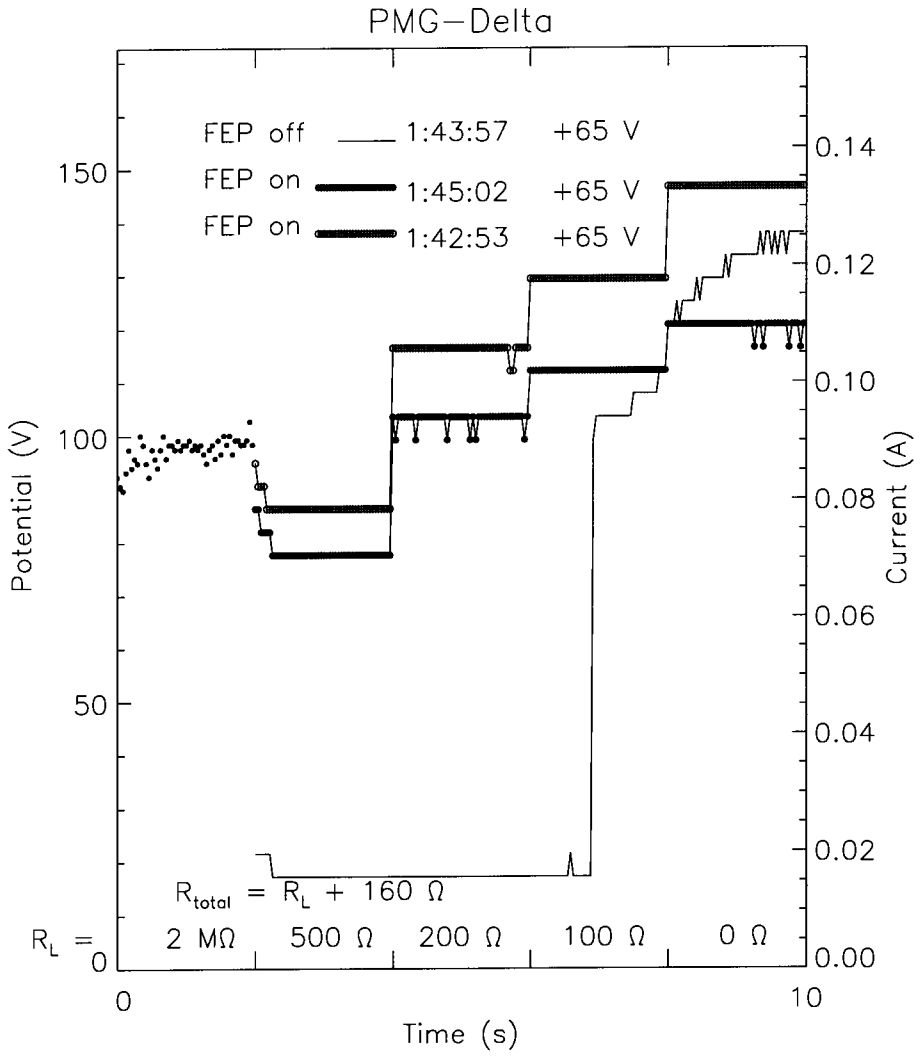

Figure 31: Current change with FEP/HCA working state

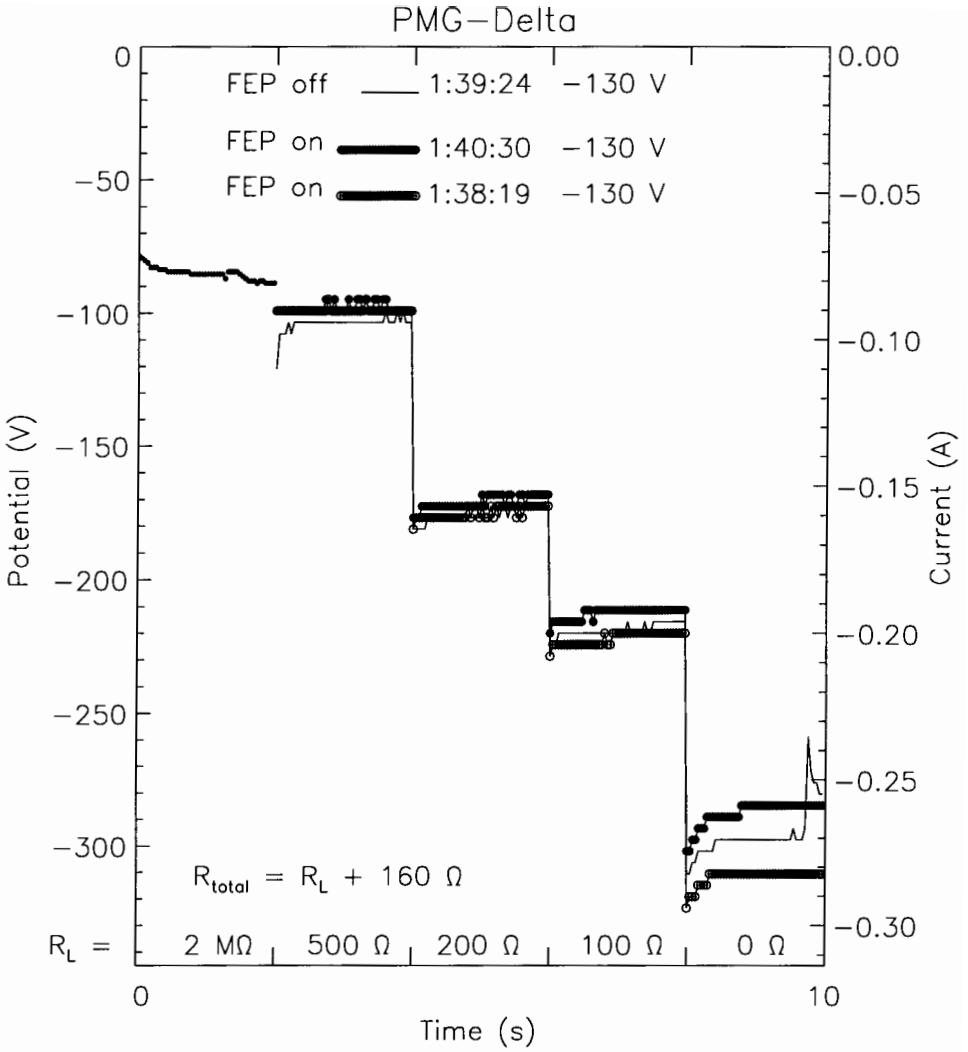

Figure 32: No current change with FEP/HCA working state

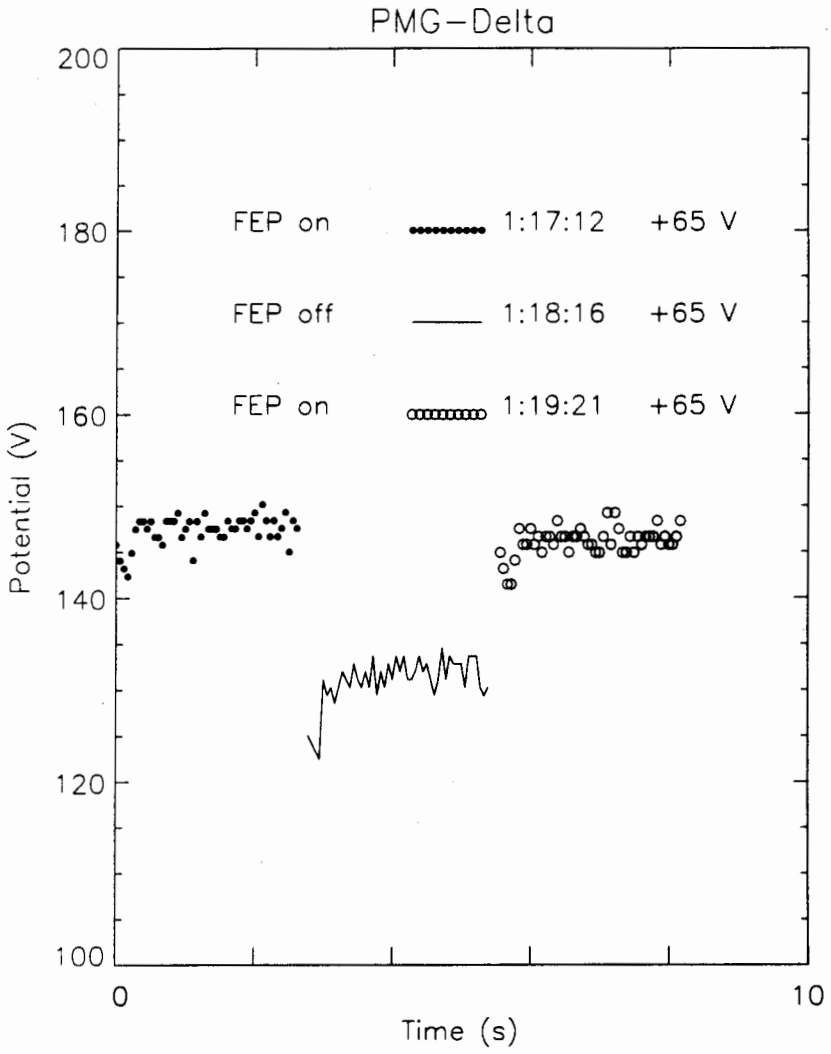

Figure 33: Potential change with HCA working condition

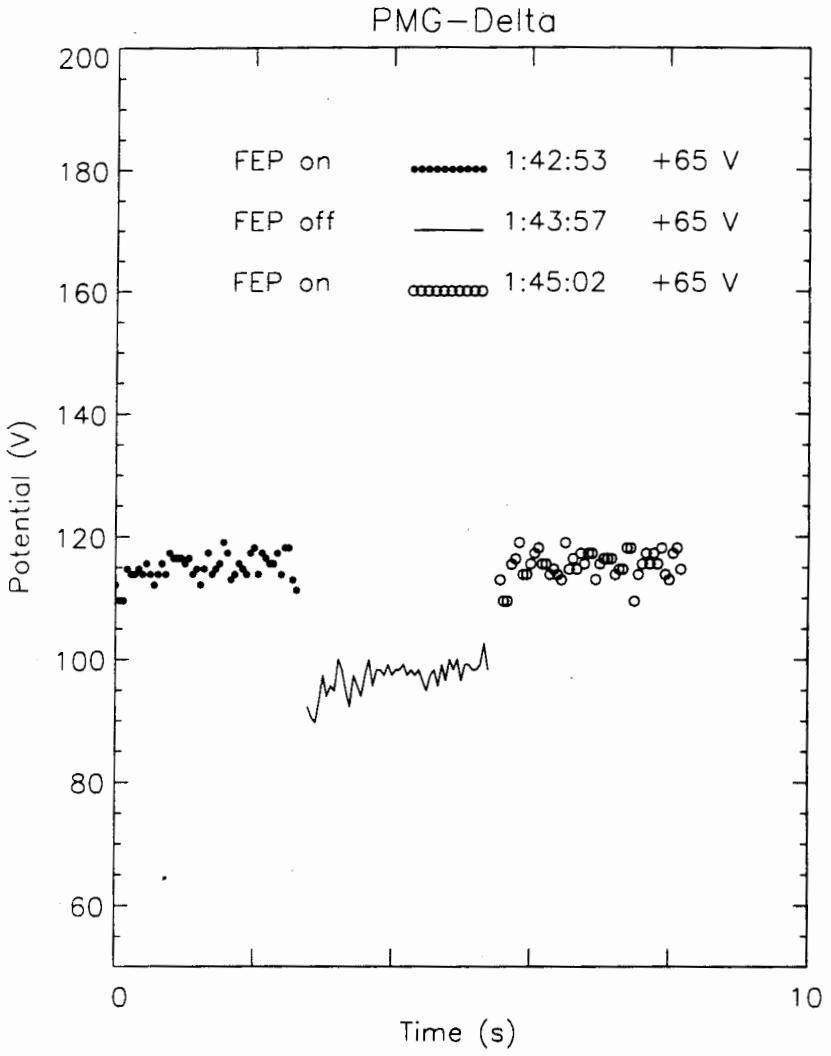

Figure 34: Potential change with HCA working condition

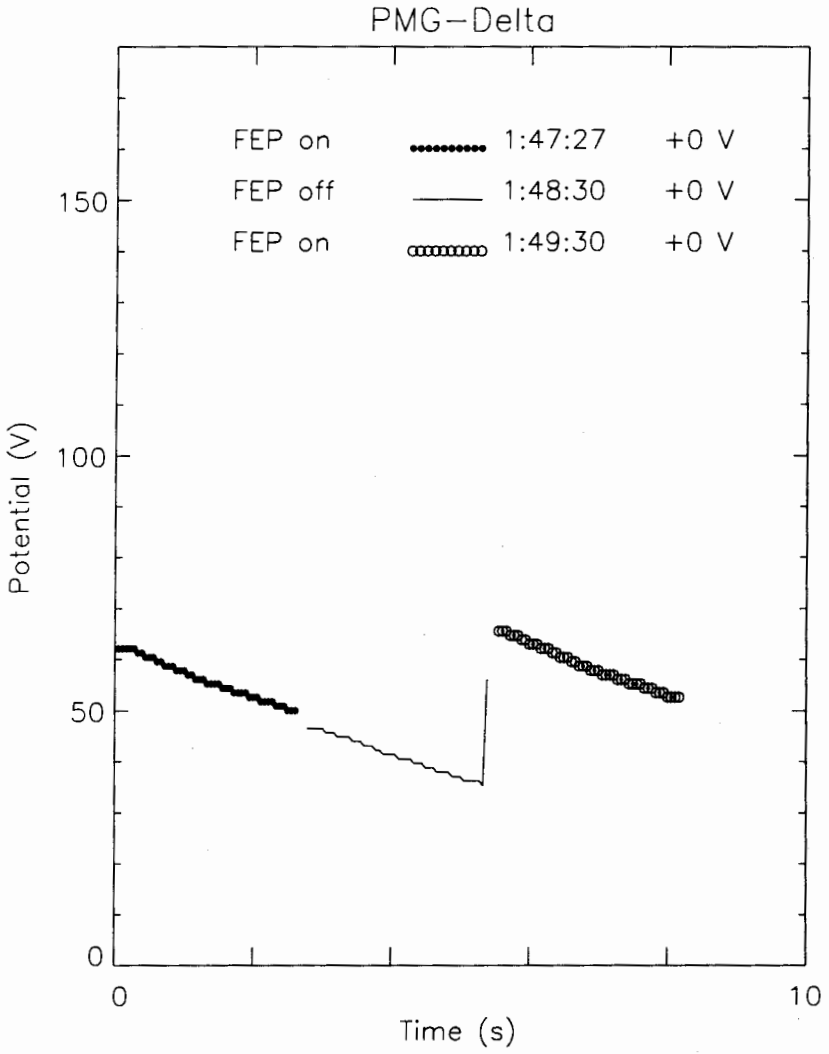

Figure 35: Potential change with HCA working condition

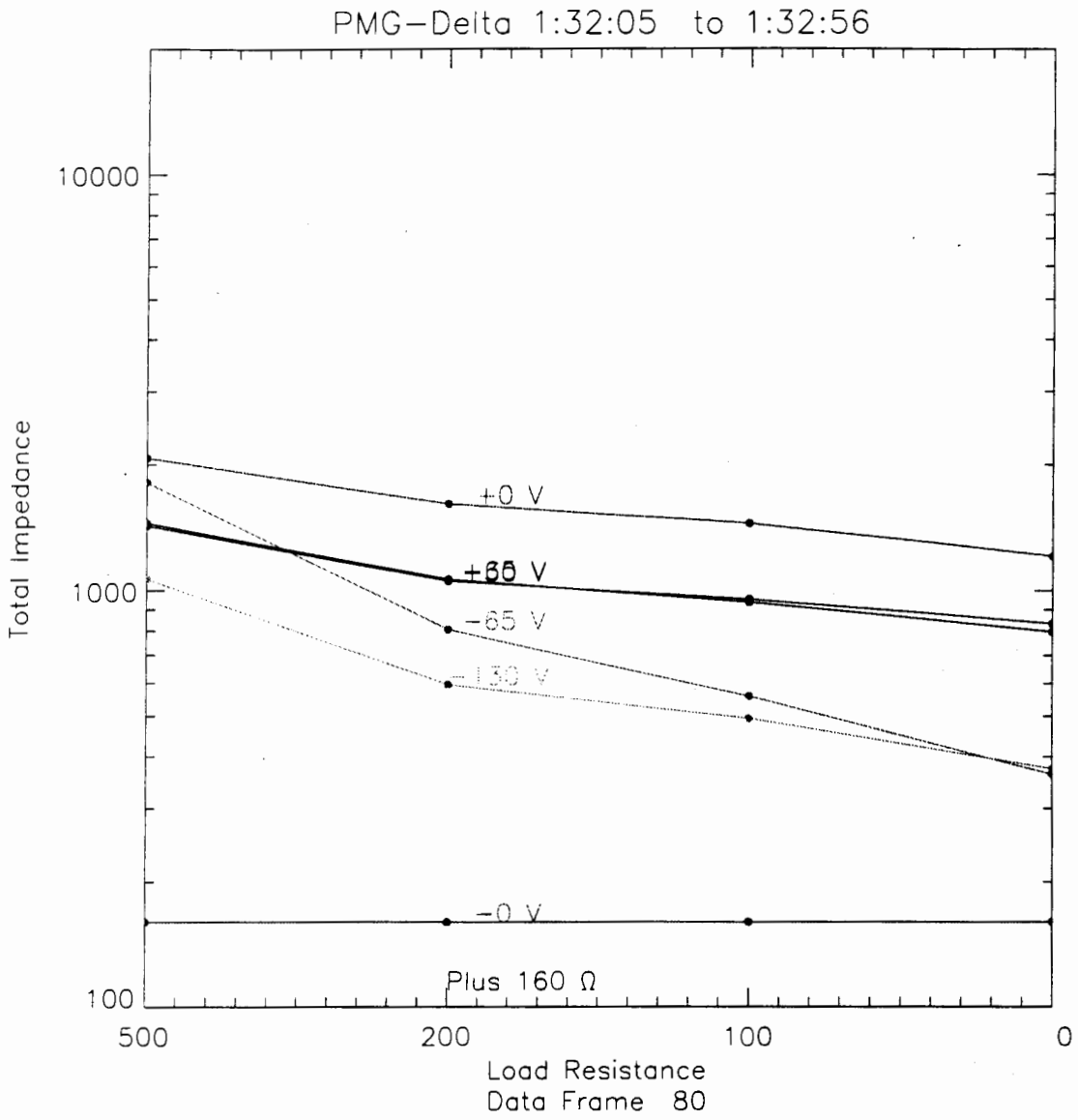

Figure 36: Plasma impedance at different bias voltage and load resistance

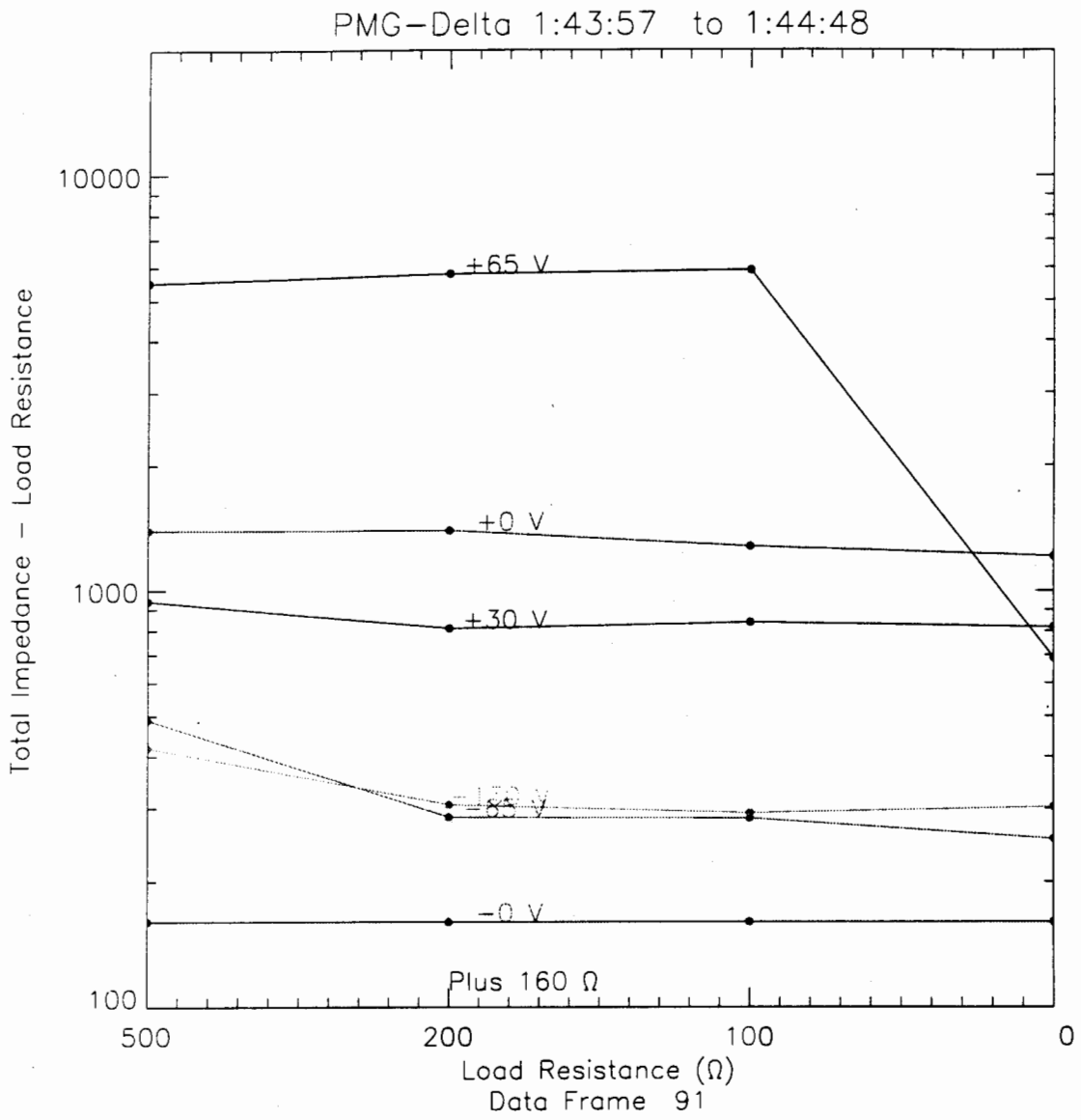

Figure 37: Plasma impedance at different bias voltage and load resistance

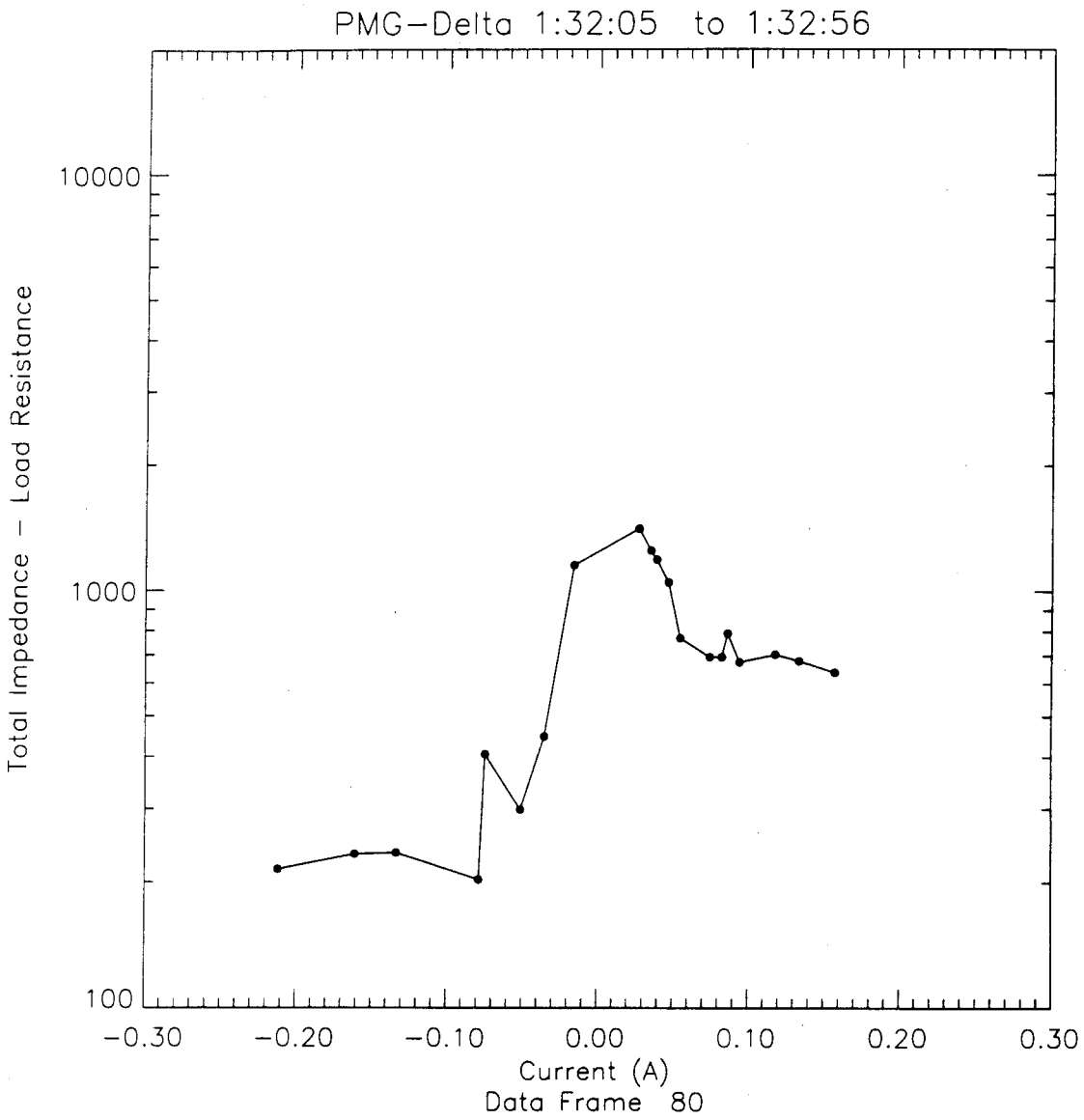

Figure 38: Impedance with current

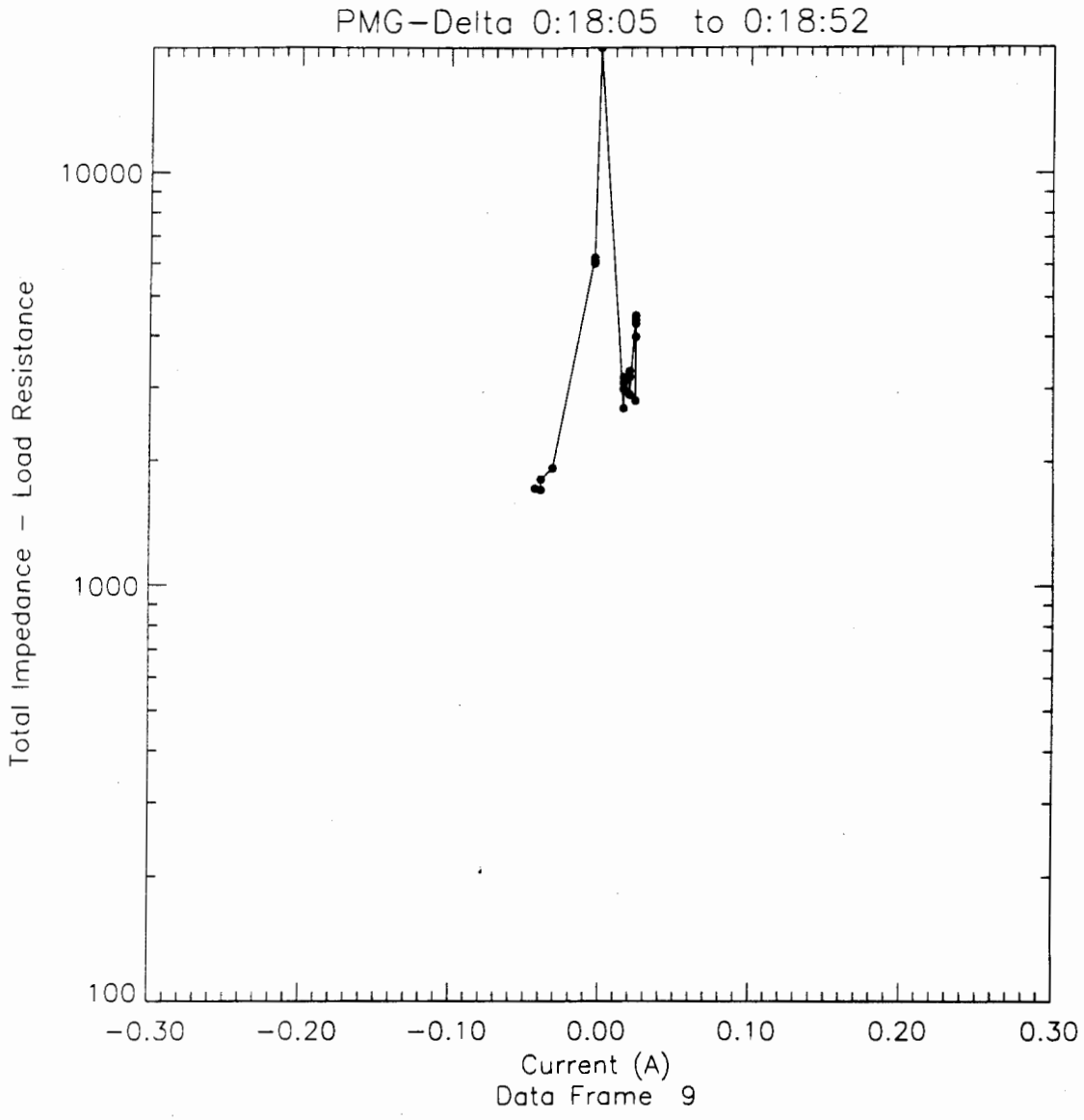

Figure 39: Impedance with current

LIST OF REFERENCES

1. David Halliday, Robert Resnick, Jearl walker, "Fundamentals of Physics", 4th ed, John Wiley & Sons,Inc.1993.

2. I. Bekey, "Tether Propulsion", Washington, D.C.; P.A.Penzo,Jet Propulsion Laboratory, Pasadena,California,1986.

3. D. E. Parks., and I. Katz., " Theory of Plasma Contactors for Electrodynamic Tethered Satellite Systems" S-CUBED, La Jolla, California, 1987.

4. Otto Heinz. and R. C. Olsen., "Introduction to the Space Environment" Naval Postgraduate School, Monterey, California, 1993.

5. A. D. Richmond, "The Ionosphere","In the Solar Wind and the Earth" edited by S. I-Akasofu, and Y. Kamide,. Terra Scientific Co, Tokyo, 1987.

6. I. Bekey, "Historical Evolution of Tethers in Space" NASA Headquarters, Washington, D.C. 1986.

7. T. D. Megna,. "Tethered Satellite System Capabilities". Martin Marietta Denver Aerospace, Denver, Co. 1986.

8. D. E. Hastings, "Theory of Plasma Contactors Used in the Ionosphere", MIT. Cambridge, Massachusetts, 1987.

9. V. K. Rawlin, and E. V. Pawlik, "A Mercury Plasma-Bridge Neutralizer" NASA Lewis Research Center, Cleveland, Ohio,1968.

10. J. W. Ward, and H. J. King,."Mecury Hollow Cathode Plasma Bridge Neutralizers", Hughes Research Laboratories, Malibu, California,1968.

11. James K. Harrison, Charles C. Rupp, (NASA) Joseph A. Carroll, Charles M. Alexander, Eric R. Pulliam,(Energy Science Laboratories, Inc.) "Small Expendable-tether Deployer System (SEDS) development status", 1989.

12. J. M. Garvey, D. R. Marin,. "Delta II secondary payload opportunities for tether demonstration experiments". McDonnell Douglas Space System Company, Huntington Beach, Califorian, 1989.

INITIAL DISTRIBUTION LIST

1.	Defense Technical Information Center Cameron Station Alexandria, VA 22304-6165	2
2.	Dudley Knox Library Code 52 Naval Postgraduate School Monterey, CA 93943-5101	2
3.	Chairman Dr. William Boniface Colson Code PH Department of Physics Naval Postgraduate School Monterey, CA 93943	1
4.	Professor Richard Christopher Olsen Code PH/OS Department of Physics Naval Postgraduate School Monterey, CA 93943	5
5.	LCDR Chang, Chung-Jen NO.173-5, Hwa-Ning road, Kaohsiung, Taiwan, R.O.C.	2
6.	Naval Academy Library P.O. Box 90175 Tsoying, Kaohsiung, Taiwan, R.O.C.	2
7.	Jerry Jost System Planning CORP 18100 Upper Bay Road, Suite 208 Houston, TX 77058	1
8.	Jim McCoy NASA/JSC/SN3 Houston, TX 77058	1
9.	Nobie Stone NASA/MSFC Huntsville, Alabama 35812	1
10.	Jim Stanley NASA/JSC Houston, TX 77508	1

11. Dr. Mario Grossi 1
SAO Center for Astrophysics
60 Garden
Cambridge, MA 02138

12. Joe Carroll 1
Tether Applications
1813 Gotham St
Chula Vista, CA 91913

13. Roy Torbert 1
Space Science Center - IEDS
Univ. of New Hampshire
Purham, NH 03824

14. Dan Hastings 1
Dept, of Aeronautics and Astronautics
MIT
Cambridge, MA 02139

15. Ira Katz 1
S-Cubed/Maxwell Laboratories
P.O. Box 1620
La Jolla, CA 92038.

16 Myron Mandell 1
S-Cubed/Maxwell Laboratories
P.O. Box 1620
La Jolla, CA 92038.

17. Victoria Davis 1
S-Cubed/Maxwell Laboratories
P.O. Box 1620
La Jolla, CA 92038
.

18. J.R. Lilley 1
S-Cubed/Maxwell Laboratories
P.O. Box 1620
La Jolla. CA 92038

19. Dale Ferguson 1
NASA/Lewis Research Center
21000 Brookpark Rd
Cleveland, Ohio 44135

20. Carolyn Purvis 1
NASA/ Lewis Research Center
21000 Brookpark Rd
Cleveland, Ohio 44135